January 2016

Notch Drives Proliferation And Radiation Resistance Of Cancer Stem Cells In Adenoid Cystic Carcinoma

Michael T. Chang
Yale University, michaelchangaccount@gmail.com

Notch Drives Proliferation and Radiation Resistance of Cancer Stem Cells in Adenoid Cystic Carcinoma

A Thesis Submitted to the

Yale University School of Medicine

In Partial Fulfillment of the Requirements for the

Degree of Doctor of Medicine

by

Michael T. Chang

2016

ABSTRACT

NOTCH DRIVES PROLIFERATION AND RADIATION RESISTANCE OF CANCER STEM CELLS IN ADENOID CYSTIC CARCINOMA. Michael T. Chang, Alex Panaccione, Beatrice E. Carbone, Christopher A. Moskaluk, Sergey V. Ivanov, Wendell G. Yarbrough. Section of Otolaryngology, Department of Surgery, Yale University, School of Medicine, New Haven, CT.

Adenoid cystic carcinoma (ACC) of the salivary gland is an indolent but highly lethal neuroinvasive tumor with a propensity for radiation resistance, recurrence, and metastasis. Molecular understanding of this rare tumor has been hampered by the absence of validated *in vitro* models and a limited number of xenografts. Therapeutic options for ACC are limited to surgery and radiation and are associated with an unacceptably low rate of cure. Cancer stem cells (CSC) are an attractive therapeutic target, and understanding their role in ACC may advance therapy. Our objectives were: 1) to establish and validate ACC cell cultures, 2) to determine if CSC exist in ACC, and if so, isolate and characterize these cells in ACC, and 3) to identify new therapeutic targets for ACC. To culture ACC and to isolate and initially characterize CSC from ACC, we modified a ROCK inhibitor-based cell culture technique, identified CD133 (PROM1) as a cell surface marker of CSCs, and used immunomagnetic cell sorting to separate and characterize RNA and protein expression in these cells. We found that CD133+ cells expressed NOTCH1 and SOX10, formed spheroids, and initiated tumors in nude mice more readily than CD133- cells. Depletion of NOTCH1 and SOX10 in cultured ACC induced death of CD133+ cells, indicating their essential roles in maintenance of stemness. An inhibitor of Notch activation, DAPT, selectively depleted $CD133^+$ cells *in vitro,* sensitized $CD133^+$ cells to radiation, and inhibited growth of ACC tumor *in vivo*. These results establish the presence of a previously uncharacterized population of $CD133^+$ cells with neural stem properties in ACC whose survival is dependent on NOTCH1 and SOX10. Sensitivity of ACC cells to Notch inhibition offer new opportunities for targeted therapy in this orphan tumor.

ACKNOWLEDGEMENTS

Foremost, I would like to thank my incredible mentor Wendell Yarbrough for his patience, encouragement, expertise, and inspiration. I would also like to express gratitude to Sergey Ivanov for his mentorship in this project. Thank you to Alex Panaccione and Bea Carbone for the camaraderie and teaching that made me excited to work each day. Thank you to Christopher Moskaluk for his collaboration. I want to thank Yale Otolaryngology, Yale Department of Surgery, and the Yale Office of Student Research for their support. Finally, thank you to my family, friends, and dearest peers, without whom any of my pursuits would not be possible.

TABLE OF CONTENTS

INTRODUCTION

Adenoid Cystic Carcinoma Overview

Background

Adenoid cystic carcinoma (ACC) comprises approximately one quarter of all salivary gland malignancies and is one of the most relentless, unpredictable, and fatal cancers of the head and neck region. First documented by French physicians Robin and Lalboulbene in their 1853 publication *Memoire sur trois productions morbides nondescrites* [Memoirs of three undescribed morbid productions], the mysterious and lethal nature of this disease was evident even in its earliest descriptions (1). In 1859, Prussian surgeon Theodor Billroth termed this disease "cylindroma," naming it for its characteristic histological appearance of cylindrical clusters of cells (2). Also noting its distinct histology, Spies is credited with coining the term "adenoid cystic carcinoma" in 1930 (3), a term popularized in the medical community in 1953 when Foote and Frazell classified several salivary gland tumor types in their seminal *Cancer* article (4). They were also the first to note that ACC spanned a wider spectrum of histological types in addition to its classic tubular appearance.

Since the earliest reports of ACC, physicians have noted several hallmark characteristics, including its tendency to involve nerves (4), recur (2), metastasize, and ultimately kill patients (5). In 1974, Conley and Dingman noted ACC to be "one of the most biologically destructive and unpredictable tumors of the head and neck" (5). Despite numerous clinical trials involving multiple treatment modalities and pharmaceutical agents over the past several decades, ACC remains a very difficult disease to treat today.

Epidemiology

While salivary gland malignancies are relatively rare, ACC represents a significant portion (22%) of these cancers (6). Worldwide yearly incidence is estimated to be 1 to 1.3 cases per 100,000 people, translating to roughly 1,200 new cases per year in the US, making ACC the second most common salivary gland malignancy overall behind mucoepidermoid carcinoma (7).

In the parotid gland, ACC is the second most commonly occurring cancer type, occurring in 7-18% of cases, however ACC is the most common cancer type in the sublingual gland (20%), submandibular gland (20%), and minor salivary glands (35-58%) lining the upper aerodigestive tract (7-10). While most often found in the minor salivary glands of the tongue, buccal mucosa, and palate (7, 9), ACC has also been reported to occur in other sites of the airways, including the paranasal sinuses, lips, larynx, trachea, and nasolacrimal tract (11). Outside of the aerodigestive tract, ACC has been reported to arise in other glandular structures, including the breast (12), prostate (13), skin (14), and female genital tract (15).

Salivary ACC typically affects people in their 5^{th} or 6^{th} decade of life, with a mean age of 57 years (16). ACC has a slight tendency to occur in females (59%), and approximately 80% of reported cases occur in Caucasians (16). Familial history, toxic exposures, or environmental exposures have not been associated with increased risk of ACC (16, 17).

Clinical Behavior

The classical behavior of ACC is somewhat paradoxical: growth is slow and indolent, but the cancer is relentless and progressive (11). Initially, ACC most commonly presents as a firm mass in the head or neck region that slowly enlarges over months to years. Depending on its location, the mass may occasionally present with pain, numbness or ulceration (18). Given its tendency to invade nerves, ACC of the parotid gland can present with facial nerve paralysis in up to one third of patients (9).

The tumor's slow growth often leaves it amenable to surgical removal, however local recurrences occur frequently, estimated in 16-39% cases (11, 18). Unlike other head and neck cancers, regional lymph node metastases of ACC to the neck rarely occur, seen in less than 10% of cases (19). However, distant metastases occur in 35-50% of cases, most commonly to the lung (20). ACC also spreads to the bones, liver, and central nervous system (20, 21). Complications resulting from distant metastases are often the cause of death, with a mean time between lung metastases detection and death of 32.3 months, and a mean time between other metastatic site detection and death of 20.6 months (22).

Diagnosis

Fine needle aspiration (FNA) is the most widely used diagnostic tool in the initial evaluation of a head and neck mass suspicious for neoplasm. Cytologic diagnosis is possible in most cases, with FNA accurately identifying about 77% of ACC cases (23). Cytologic analysis for ACC typically shows basaloid tumor cells clustered around globules containing eosinophilic extracellular matrix material (23). Clinicians must be

careful to distinguish ACC from pleomorphic adenoma, the most common benign tumor of the salivary gland, as the two can have a very similar cytologic appearance. Largely because of the cytologic similarity between ACC and benign tumors, the false negative rate for FNA is 17%, therefore clinicians must interpret FNA results in the context of other clinical findings (23).

Radiographic imaging by computed tomography (CT) or magnetic resonance imaging (MRI) is used for evaluating the extent of tumor spread. MRI with gadolinium contrast is important in assessing for nerve involvement. ACC tumors tend to have poorly defined borders and homogeneous enhancement on T1-weighted MRI imaging, however there are no objective radiographic signs specific to ACC versus other salivary tumor types (24). Final diagnosis is made from histopathological analysis of a resected specimen.

Histopathology

ACC is composed of two cell types within the salivary gland: myoepithelial cells and ductal cells (9). Classically, there are three histological subtypes of ACC: cribiform, tubular, and solid. Cribiform is the most common histology and is predominantly composed of "punched out" pseudocysts amongst small ductal cell islands. Tubular histology shows a palisading pattern of well-formed ducts lined by myoepithelial cells. Solid histology involves solid sheets of both cell types with thin strands of intervening stroma. Solid histology has historically been associated with a worse prognosis (25); however, later studies have shown that tumor stage rather than histologic grade is a more accurate prognostic indicator (26). While classically these histological subtypes have

been viewed as distinct, the majority of tumors contain a mixture of these patterns (9). In all subtypes, perineural invasion is very common (60% of cases), even in early stage tumors (27).

Immunohistochemical (IHC) stains aid in the diagnosis of ACC. Characteristic expression for ACC includes carcinoembryonic antigen (CEA), muscle specific actin (MSA), Ki-67, and several cytokeratins (28). ACC stains very similarly to another low-grade cancer, polymorphous low grade adenocarcinoma (PLGA); however, cellular atypia and high Ki-67 index can assist in identifying ACC (9). Despite the histological appearance of a low-grade cancer, all cases of ACC are considered high-grade salivary gland neoplasms given the aggressive clinical behavior.

Management

For ACC of a major salivary gland, surgical excision of the entire involved gland is the primary treatment option. Treatment of minor salivary gland tumors depends on location, with oral cavity lesions typically being excised and lesions closer to the skull base undergoing endoscopic removal or gamma knife therapy. Negative margins are important to obtain, as margin status has been shown to be a significant predictor of local recurrence (29). Interestingly, however, margin status has no significant bearing on rate of distant metastasis (29). Because regional lymph node metastases are relatively rare in ACC, neck dissections are typically reserved for cases where there is clinical evidence of neck node metastasis (19).

Postoperative radiotherapy is often employed, as studies have shown it to significantly improve local control for both early and late stage tumors (27); however,

opposing studies have found that postoperative radiation does not significantly affect local control except in advanced stages or cases with positive margins (30, 31). Importantly, the addition of radiation has no significant effect on rates of distant metastasis or overall survival (27, 30). Despite treatment with postoperative radiotherapy, radiation resistance remains an issue as local recurrence occurs in approximately one-third of cases (11, 18).

To date, no systemic agents have been shown to induce a significant response in the treatment of ACC, thus chemotherapy is typically reserved for palliative measures in unresectable or metastatic disease (32).

Prognosis

The 5-year overall survival is 85-90%, however the 15-year overall survival rate is 35-40% (25, 27, 30), reflective of a protracted clinical course typical of ACC. Factors associated with worse prognosis include positive resection margins, major nerve involvement, and advanced stage (27, 33). While it is possible for patients to live many years with this indolent cancer, long-term disease-free survival is dismal being only 42% at 5 years and 29% at 10 years (34). The majority of ACC cases end with death resulting from complications of metastatic disease (22).

Molecular Landscape of ACC

Mutational Profile

Because the molecular drivers of ACC remain largely unknown, next-generation sequencing methods have been employed to elucidate its mutational landscape. Three

recent studies performed genome and whole exome sequencing, looking at a combined 108 ACC specimens with matched normal DNA (35-37). All studies found a very low somatic mutation rate, with one analysis reporting 13 mutations per exome (35), and another study reporting a mean of 22 somatic mutations per sample, correlating to a non-silent mutation rate of 0.31 mutations per megabase (36). ACC was also found to have a highly diverse mutational profile, with mutations seen in chromatin state regulators, DNA damage pathways, and growth factor signaling.

All studies identified t(6;9) fusions of the MYB-NFIB genes, as well as somatic mutations in the MYB gene, aberrations seen in the majority of ACC cases (38). The t(6;9) MYB-NFIB fusion has historically been the most commonly cited marker of ACC, as it is unique to this tumor compared with other head and neck cancers (38). Recently, a t(8;9) fusion of another MYB family member, MYBL1, and NFIB has been identified in approximately 30% of t(6;9)-negative cases (39). MYB is a transcription factor with a plethora of targets and acts to both activate and inhibit transcription of its targets. Activation of MYB has several downstream effects including cellular proliferation and inhibition of terminal differentiation, thus it is hypothesized that the translocation induces pathologic changes of these cellular processes (40). MYB alterations have a significant association with recurrence and metastasis (39), and the common presence of mutations and fusions of MYB family members suggest that activation of this pathway is critical, if not required, in development or maintenance of ACC.

Whole exome sequencing also found mutations in the FGF/IGF/PI3K pathway in 30% of cases (36). Moreso, samples with phosphatidylinositol 3-kinase (PI3K) mutations were all from solid histology tumors, traditionally seen as the most aggressive variant of

ACC. Fibroblast growth factors (FGF) and insulin-like growth factors (IGF) are known to be potent oncogenic activators of PI3K (41). Further research into this pathway may present a potentially promising therapeutic target for a subset of ACC cases.

Expression Changes

To identify differentially expressed genes involved in ACC formation or maintenance, microarray gene expression analyses surveyed 8920 genes in 15 ACC specimens and 5 normal salivary glands (42). Given the myoepithelial origin of the tumor, it was not surprising that several genes involved in myoepithelial differentiation are upregulated in ACC. Notable genes that are highly overexpressed included SOX4, a transcription factor involved in neural and immunologic cell development, AP-2γ, an upstream effector of oncogene c-Kit, and casein-kinase 1ε and frizzled-7, both members of the Wnt/β-catenin pathway (42).

IHC examination of 27 ACC specimens found c-Kit (CD117) overexpression in 90% of ACC cases (43). c-Kit is a tyrosine kinase receptor involved in numerous physiologic processes including hematopoiesis, spermatogenesis, and cell migration (44) and is a transcriptional target of MYB (45). c-Kit is a known oncogenic driver in other types of cancers such as seminomas and gastrointestinal stromal tumors (GISTs) (46, 47), and c-Kit inhibition results in dramatic regression of GISTs (48). In ACC, c-Kit levels are associated with poorer prognosis (43). Interestingly, c-Kit has been used to isolate salivary progenitor cells, suggesting it may play a role in stem cell maintenance in ACC. Though initially promising, however, tyrosine kinase inhibitors of c-Kit have failed to

induce a therapeutic response in several clinical trials treating patients with ACC (49, 50).

SOX10, a transcription factor required for maintenance and migration of neural crest stem cells, is also highly expressed in both primary ACC specimens and ACC xenografts compared with normal salivary tissue and other salivary tumor types (51). Microarray analyses indicating high SOX10 expression in ACC was confirmed by IHC. *In silico* analysis identified genes co-expressed with SOX10 and defined the SOX10 gene signature as unique to ACC compared with other salivary gland malignancies (51). Interestingly, SOX10 is also expressed in basal-type breast carcinoma specimens as confirmed by IHC, and components of the larger SOX10 gene signature are preserved in basal-like breast cancers. The required role for SOX10 in neural crest stem cells, the derivation of myoepithelial cells from neural crest, and the involvement of myoepithelial cells in ACC and basal-like breast cancer suggest that SOX10 may play a critical role in supporting the stem cell features in ACC and a subset of breast cancer, as well as other cancers containing neural crest derivatives (51).

Fatty-acid binding protein 7 (FABP7), normally a chaperone for lipids between cytoplasm and nucleus, is part of the SOX10 signature and is highly overexpressed in microarray studies of ACC xenografts versus normal salivary glands (52). In ACC, FABP7 is highly expressed in myoepithelial cell nuclei, suggesting a potential role in development or proliferation of ACC, as nuclear FABP7 is present in rapidly proliferating cells of other cancers (53, 54). Although the precise role of FABP7 in ACC development or maintenance is not known, its expression correlates with aggressive behavior and poor prognosis in ACC (52). In other cancers of neural crest derivatives

such as glioma, FABP7 has been implicated as a critical player in stem cell maintenance (55), and the presence of nuclear FABP7 is associated with poorer prognosis compared to cytoplasmic FABP7 (53). The biological consequences have not been well characterized, however FABP7 has been identified as a target of Notch signaling (56). As understanding of the Notch pathway in ACC becomes better understood, so may the role of FABP7.

Epigenetic Alterations

Given the overall low mutational load in ACC and the relatively high number of mutations involving chromatin regulators (37), it is likely that epigenetic changes play critical roles in driving ACC. Analysis of CpG island DNA methylation levels in 16 ACC specimens with matched normal tissue (57) revealed hypermethylated genes including initiators of apoptosis or differentiation such as BCL2L11, transcription factors such as EN1, GBX2, FOXL1, and NR2F2, and effectors of metabolism including XRN2, INSRR, and PNLIPRP1, suggesting that epigenetic silencing of these genes may play an important role in ACC. Significant hypomethylated genes in ACC include DOCK1, involved in cell surface extension, and PARVG, involved in cell adhesion (57). The biological consequences of these epigenetic changes require further study to determine their functional significance and possible therapeutic implications.

Notch Signaling in ACC

Notch signaling is a highly conserved pathway that mediates cellular differentiation and growth. Canonical Notch signaling is initiated by five ligands, Delta-like 1 (DLL1), DLL3, DLL4, Jagged-1 (JAG1), and JAG2 that bind to Notch receptors

and trigger proteolytic cleavage by gamma-secretase. Notch cleavage releases the Notch intracellular domain (NICD) that translocates to the nucleus where it imposes its regulatory activity as a transcription factor (58). NOTCH can serve as an oncogene like it does in breast cancer and T-cell acute lymphoblastic leukemia (58, 59), or as a tumor suppressor, like in squamous cell carcinoma of the head and neck (HNSCC) (60). The specific role of Notch signaling in ACC has yet to be fully elucidated.

Gene expression comparison between ACC and normal salivary tissue identified that several genes in the Notch signaling pathway such as NOTCH3 and JAG1 were highly expressed in cancers (42). In addition, NOTCH1 mutations were found in ACC xenografts (58), and these exonic mutations are known to induce ligand-independent release of NICD or stabilize the active NICD through deletion of the C-terminal PEST domain. Interestingly, NOTCH1 activation, as measured by NICD, predicts response to gamma-secretase inhibitors in breast cancer and ACC models (58). Further supporting a role for Notch activation in ACC, whole exome sequencing identified missense or truncating mutations in NOTCH1 and NOTCH2 in a low number of primary tumors, though functional consequences of these NOTCH mutations were not determined in these particular cases (35). As the role of Notch signaling in ACC becomes clearer, more therapeutic opportunities for ACC may open, especially as Notch inhibition becomes an increased focus of pharmaceutical companies.

In Vitro and *In Vivo* Tools for ACC Research

Cell Lines

Particularly in rare cancers where original tumor tissue is scarce, reliable *in vitro* models can play a critical role in the study of its molecular and biological properties, as well as testing of potential therapeutic agents. At one point, several cell lines exchanged by many academic institutions were used to study ACC, including ACC2, ACC3, ACCM, ACCS, ACCNS, and CAC2. However, in 2009, short tandem repeat (STR) DNA fingerprint analysis examining eight loci of nucleotides was performed with cross-referencing of these lines with national databases (61). Unfortunately, all six cell lines were either improperly identified as ACC or contaminated. ACC2, ACC3, and ACCM were found to be HeLa cells, ACCS were T24 urinary bladder cancer cells, ACCNS were mouse cells, and CAC2 were rat cells (61). Misidentification of these cell lines nullified the validity of all work derived from these cell lines, and since then, researchers have had a great need for new *in vitro* tools to study ACC.

After the devastating results disqualifying previous ACC cell lines, another cell line, SACC-83, derived from a minor salivary gland cancer has been described. Passage of this cell line through a mouse was used to derive a line with higher metastatic potential, SACC-LM (62, 63). STR analysis has shown that these cells are distinct from HeLa cells, however a comparison with public databases has yet to be reported to ensure a unique signature. Additionally, distribution of these cell lines has been very limited outside of China.

In 2014, an additional cell line, MDA-ACC-01, was developed from a base of tongue ACC (64). STR analysis indicated a unique phenotype and early cultures

proliferated well. However MDA-ACC-01 began to senesce after passage 7, requiring immortalization with human telomerase transcriptase. Additionally, the properties of cultured cells may differ from those of the original tumor, with loss of the known MYB-NFIB translocation reported in later passages of this cell line (64).

Patient-Derived Xenografts

Several patient-derived xenograft (PDX) models of ACC were developed and have been distributed to several research groups focused on ACC (65). Patient tumor tissue was successfully propagated in the subcutaneous flanks of immune deficient nude mice in 17 of 23 attempts (74%). Tumors were confirmed to be ACC by histologic analysis, IHC characterization, gene expression profiling, and the detection of the MYB-NFIB fusion. Karyotype profiling confirmed that xenografted tumors were derived from the parent tumor (65).

In addition to serving as reliable preclinical models of disease, xenografts also serve as a way to expand available tumor tissue, which is particularly useful in rare cancers like ACC. However, PDX models have their limitations in research, namely increased maintenance cost, facility space, and distribution difficulty. Furthermore, PDX models do not offer the same ability to manipulate gene expression or to perform high throughput screening compared to cell culture.

Clinical Trials

Systemic Single-Agent Cytotoxics

Because recurrence and metastasis occur frequently despite surgery and radiation, multiple clinical trials have been undertaken to assess the utility of systemic therapy in ACC. Despite over 30 phase II clinical trials enrolling patients with ACC since 1985, no successful single-agent or combinatorial regimens are approved for ACC treatment (32).

Single-agent treatments with traditional cytotoxic drugs have largely failed to achieve objective responses. In eight trials of single-agent cytotoxic regimens of gemcitabine (66), paclitaxel (67), cisplatin (68, 69), mitotraxone (70, 71), epirubicin (72), and vinorelbine (73), major objective responses occurred in 18 of 141 (12.8%) of patients with recurrent and/or metastatic disease (32). For those cases that did respond to treatment, durations of response were short, ranging from 5 to 20 months. Of all single-agent therapies, platinum-based regimens with cisplatin were most effective, achieving an objective response in 2 of 13 patients, though the reported durations of response were a short 5 and 8 months (69). Disease stabilization was a more common finding in these trials, reported in 64 of 111 (57.7%) patients (32). However, durations of effect were again short, with a maximum reported stabilization period of 30 months. Furthermore, in ACC it can be difficult to distinguish treatment-induced disease stabilization given the indolent natural course of the disease. In recognition of this point, some trials have begun documenting ACC progression status before initiation of therapy.

Combinatorial Cytotoxic Regimens

Combinatorial regimens of traditional cytotoxic agents have also failed to produce broad sustained effects. A review of 17 trials of combinatorial chemotherapy found that 35 of 143 (24.5%) cases demonstrated an objective response (32). Cisplatin and doxorubicin were most commonly tested, and they were employed in combination with cyclophosphamide in four trials (74-77). These trials reported the highest objective response rates occurring in 9 of 36 (25%) patients; however duration of response was short, ranging from 5 to 16 months (75, 77). Though results were slightly better than single agent trials, combinatorial cytotoxic therapy also failed to achieve sustained responses. Higher rates of toxicity were also seen in combinatorial compared to single-agent therapy (73).

In addition to lack of prolonged response time, another major issue with standard cytotoxic treatment is the lack of broad effectiveness. Because of the rarity of ACC, large patient trials are very difficult to organize, and it is thus difficult to perform subset analyses to reliably identify patient or clinical characteristics predicting response. Despite failure to induce objective responses, chemotherapeutic agents still play a significant palliative role in ACC management, with symptomatic relief reported in 30-70% of single-agent treatments and 25-64% of combinatorial regimens (32).

Molecularly Targeted Therapies

Given the discovery of high c-Kit expression in 90% of ACC tumors, imatinib, a tyrosine kinase inhibitor (TKI), has undergone multiple trials with the aim of blocking c-Kit signaling. Six trials of have assessed imatinib activity in a cumulative 71 ACC

patients, five of which found zero objective responses (49, 50, 78-80) and one of which saw two objective responses (79). One trial also assessed the effect of adding cisplatin to imatinib, reporting three patients with partial responses in the combination group versus none in the imatinib only group (81).

As in other cancers, epidermal growth factor receptor (EGFR) is overexpressed in ACC and has been correlated with tumor grade (82), prompting the trial of EGFR inhibitors. Gefitinib, the first inhibitor of EGFR's tyrosine kinase domain, was studied in 18 patients with recurrent and/or metastatic ACC, but no objective responses were seen (83). Lapatinib, a TKI targeting EGFR and erbB2, was tested in 19 patients with ACC positive for EGFR and/or erbB2. No objective responses were reported, but nine patients (47%) had disease stabilization lasting more than 6 months (84). Cetuximab, a monoclonal antibody inhibitor of EGFR, was trialed in 23 patients with recurrent and/or metastatic ACC (85). No responses to therapy were observed, but eight patients (35%) had a disease stabilization lasting a median time of 4.5 months (85). Another study trialed cetuximab plus cisplatin and 5-fluorouracil (5-FU) chemotherapy in 12 patients with metastatic EGFR-positive ACC and cetuximab plus cisplatin with concomitant radiotherapy in nine patients with locally advanced EGFR-positive ACC (86). Compared to historical outcomes, results were favorable, with objective responses occurring in four (44%) patients with locally advanced disease and five (42%) patients with metastatic disease (86). These results suggest that regimens combining biologic inhibitors, platinum-based chemotherapy, and radiotherapy may be a viable treatment approach in ACC.

Studies of ACC have shown mutations and an overexpression of members in the fibroblast growth factor receptor (FGFR) signaling pathway (35, 36), warranting testing

of fibroblast growth factor receptor inhibition. A recent phase II study has assessed the efficacy of oral dovitinib, a multi-kinase inhibitor of FGFR, vascular endothelial growth factor receptors (VEGF), and platelet-derived growth factor receptors (PDGFR), in 32 patients with unresectable or metastatic ACC (87). There were no complete responses, one partial response (3%), and 30 cases (94%) with disease stabilization, though the authors note that it was difficult to determine if these cases were truly results from treatment rather than natural disease course (87).

Sunitinib has been another drug of interest, given its ability to inhibit multiple targets identified as critical in ACC, including c-Kit, VEGF, PDGF, and the RET oncogene. A phase II study studied the efficacy of sunitinib in 13 patients with progressive, recurrent, or metastatic ACC (88). Again, however, no responses were seen, while 11 patients (85%) demonstrated disease stabilization (88).

Bortezimib, an inhibitor of the 26S proteasome and thought to function at least partially through inactivation of NF-kB, has been studied as a single-agent and in combination with doxorubicin in a phase II trial of 24 patients with progressive or metastatic ACC (89). Though well tolerated, no objective responses were seen in either treatment group, and only one partial response was seen in the combination group (89).

mTOR, a master cell growth regulator and target of PI3K, has been implicated as an ACC driver and inhibition in preclinical trials have induced cell death in ACC (90), prompting a phase II study of everolimus, an mTOR signaling inhibitor. Out of 34 patients with progressive unresectable ACC, 27 patients (79%) showed disease stabilization, however no responses were observed (91). As toxicities were very well tolerated, mTOR inhibition may play a role in controlling unresectable disease; however,

the caveat of determining efficacy based on disease stabilization in indolent tumors remains.

Current Trials

Several preclinical trials have shown promise with regard to potential molecular targets and are prompting more phase II clinical trials that are currently ongoing. Agents under investigation include selinexor (inhibitor of CRM, EGFR, HER2, FGFR, c-Kit), eribulin (inhibitor of mitosis), pembrolizumab (PD-1 inhibitor), and vorinostat (histone deacetylase inhibitor).

Despite numerous trials with small molecule inhibitors, inducing a reliable response in ACC remains elusive. While several of the agents studied achieved stable disease states lasting more than 6 months, more long-term follow up is required to determine control of late disease progression, given the naturally protracted course of ACC.

The poor track record of clinical trials using cytotoxic or targeted agents in ACC likely represents inherent resistance of these cells and point to the inadequacy of pre-clinical studies to predict response. Clearly, understanding of the true molecular drivers of ACC remain poor, suggesting that new tools for study and biologic innovation is needed to make therapeutic advances in ACC. A potentially exciting area of investigation is the role of Notch in ACC. Building off recent data implicating Notch importance in ACC (35, 42, 58), three phase I clinical trials studying the efficacy of Notch inhibitors in ACC are underway (92). One trial is investigating the efficacy of brontictuzumab (OMP-52M51), a monoclonal antibody against the Notch1 receptor in refractory and recurrent

cases. Two independent trials are assessing the efficacy of BMS-906024, a new pan-Notch inhibitor, with one study utilizing it as a single-agent and the other in combination with traditional chemotherapy (92).

Cancer Stem Cells

Cancer Stem Cell Theory

An emerging concept in oncologic treatment is targeting of cancer stem cells (CSC), a subpopulation of self-renewing tumor cells capable of reinitiating and recapitulating all cells within the tumor (93). Because radiotherapy and traditional chemotherapeutics tend to target rapidly proliferating cells, the relatively quiescent state of CSC may allow them to evade these treatments and thus cause recurrent or metastatic disease. CSC have been identified in multiple cancers, including myeloid leukemia (94), HNSCC (95), colorectal (96), pancreatic (97), and neurologic cancers (98). Typical markers used to identify stem-like cells include aldehyde dehydrogenase 1 (ALDH1) (99), aldehyde dehydrogenase activity (100), CD44 (95), CD34/CD38 (94), and CD133 (96).

Cancer Stem Cells in ACC

Preliminary evidence suggests that ACC may contain cancer stem cells. One study isolated cells with high expression of ALDH1 ($ALDH1^{high}$) from cells with low expression of ALDH ($ALDH1^{low}$) in primary ACC tumors and ACC xenografts (101). Injection of these separated cells into NOD/SCID mice revealed that $ALDH1^{high}$ cells are more tumorigenic (24 of 60 tumors formed) compared with $ALDH1^{low}$ cells (5 of 126

tumors formed). Tumors formed from ALDH1^{high} cells maintained histological patterns reminiscent of clinical ACC specimens (101). Interestingly, ALDH1^{high} cells formed spheroids characteristic of stem cells seen in other neurologic cancers such as neuroblastoma (98). Given that ACC highly expresses common stem cell markers and shares expression profiles with other neurologically based cancers (51), ACC may be similarly driven by stem cells with neurologic or neural crest properties.

Notch in Cancer Stem Cells

Notch has been identified as a critical mediator of CSC maintenance in many other cancer types including breast cancer (102), pancreatic cancer (103), embryonal brain tumors (104), and gliomas (105). The strongest evidence of Notch involvement in stemness maintenance is seen in breast carcinoma and glioblastoma cell lines, where blockade of Notch signaling by gamma secretase inhibition decreases the formation of spheroids containing stem-like cells (105, 106). Notably, gamma secretase inhibition specifically increases radiation-induced death of glioma CSCs while having relatively little effect on glioma bulk cells (107). In pancreatic cancer, Notch activation is associated with gemcitabine-resistant cells (108). These encouraging studies suggest that targeting of CSCs via Notch inhibition may have a potential role in treatment of radiation-resistant and chemo-resistant cancers, including ACC.

While still a preliminary hypothesis, the presence of a stem-like population in ACC may, in part, be responsible for its high rate of recurrence and metastasis. Selective targeting of critical molecular mediators in this subpopulation may be a promising new approach in ACC treatment.

STATEMENT OF PURPOSE

Hypothesis

Salivary ACC contains a subpopulation of cells with neural CSC-like properties driven by NOTCH1, SOX10, and FABP7 signaling. Inhibitors of Notch signaling may be effective in preventing CSC growth and radiation resistance, and thus has potential therapeutic relevance in ACC.

Aims of this Study

1. Establish and validate ACC cell cultures.

Recent studies have found that existing ACC cell lines were contaminated or misidentified and did not represent ACC (61). We aim to establish and verify new ACC cultures from ACC xenografts and patient tumors, and if possible establish immortalized cell lines so that functional experimentation can be performed to better understand ACC biology.

2. Identify, isolate, and characterize CSC from ACC specimens.

We aim to build on existing studies suggesting the presence of CSC in ACC and identify markers to distinguish and isolate the CSC population. After isolating this population of cells, we will characterize their behavior and expression profile to assess for potential drivers.

3. Elucidate role of NOTCH and other molecular drivers of CSC in ACC.

We aim to perform functional assays to determine potential roles and interaction of NOTCH, SOX10, and FABP7 in maintenance of CSC, and the mechanisms by which these mediators operate.

4. Assess therapeutic role of NOTCH inhibition in ACC.

Based on insights gained from *in vitro* studies of Notch signaling, we aim to evaluate the efficacy of Notch signaling inhibitors in the prevention of ACC tumor growth in culture and animal models. Additionally we assess the effect of Notch signaling inhibition on the ability of ACC cells to resist radiation.

METHODS

PDX and Primary Tumor Specimens

Validated PDX models of ACC were obtained from Christopher Moskaluk at the University of Virginia (65). An additional clinical ACC specimen (ACC33) was collected from the Smilow Cancer Center at Yale New Haven Hospital, obtained through written patient consent and with approval from the Yale Institutional Review Board (HIC# 1206010419).

Tissue Processing

5-10 mg of fresh or cryopreserved (90% FBS and 10% DMSO) tumor tissue underwent separate rinses with PBS, 70% EtOH, 100X Anti-Anti (GIBCO), and PBS

containing 1:500 ceftazidime. Tumor tissue was subsequently minced and transferred to a 15mL plastic tube for digestion at 37ºC for 1-2 hours with occasional agitation. Digestion mixtures were comprised of 3 mL of complete DMEM media (DMEM with 10% fetal bovine serum (FBS), 1X Penicillin-Streptomycin, 1X L-Glutamine) supplemented with 1 mL of dispase (BD Biosciences, San Jose, CA), 30-150 μL hyaluronidase (Sigma, St. Louis, MO), and 30-150 μL collagenase (Roche, Indianapolis, IN). Digested tissue was collected at 1,500 RPM for 3 minutes, rinsed with PBS, re-centrifuged, transferred into 3 mL of F+Y culturing media (see below), and filtered using a 100 μm cell strainer. Tumor cells were then transferred to T-12.5 or T-25 flasks, depending on tumor volume, for culturing. Tumor cells were cultured together with either irradiated 3T3-J2 mouse fibroblast feeder cells or conditioned media derived from these cells (see below). Tissue processing was performed by both Michael Chang and Alex Panaccione.

Cell Culture

To establish a reliable ACC culture protocol, we modified a recently published epithelial cell culturing technique using Rho-kinase (ROCK) inhibitor and irradiated 3T3-J2 mouse fibroblasts serving as feeder cells (109). Feeder cells were cultured in complete DMEM media and grown to confluency in T-175 flasks. Upon reaching confluency, cells were trypsinzied, washed, collected, and resuspended in fresh complete DMEM media. Feeder cells were irradiated with 30 Gy, counted, and immediately stored at 4^{o}C for use up to 36 hours post-radiation. To create feeder cell conditioned media, irradiated 3T3-J2 cells were incubated in a T-150 flask supplemented with 30 mL of DMEM media for 4 days. Media was filter-sterilized and then mixed in a 1:4 ratio with F+Y culturing media.

F+Y culturing media contained 373 mL DMEM mixed with 125 mL F12 media (Life Technologies) that contained 7.5% FBS (Life Technologies), 10 ng/μL EGF, 5 μg/mL insulin (Sigma, St. Louis, MO), 250 μg/mL amphotericin (Fisher Scientific, Pittsburgh, PA), 10 mg/mL gentamicin (Life Technologies), 8.6 ng/mL cholera toxin (Sigma), and 10 μM Y-27632, a ROCK inhibitor (Enzo Life Sciences, Farmingdale, NY). Cultured cells were derived from both PDX and patient tumor tissue. Cell culture work was performed by both Michael Chang and Alex Panaccione.

Microsatellite Analysis

To authenticate cell cultures and cell lines, we used the Promega GenePrint 10 STR analysis PCR kit with fluorescent tagging. PCR products were analyzed on Applied Biosystems 3730xL DNA Analyzer at the Yale Keck Facility and data was processed using GeneMapper 3.7 software (Applied Biosystems). The results were cross-referenced with publically available STR databases to ensure unique STR signature (http://www.cstl.nist.gov/strbase/, http://www.dsmz.de/services/services-human-and-animal-cell-lines/online-str-analysis.html). Microsatellite analysis was performed by Bea Carbone with assistance from Michael Chang and Alex Panaccione.

Real-time RT-PCR

To assess RNA transcript levels, RNA was isolated from frozen cell pellets of cells using RNeasy kit (Qiagen, Valencia, CA). cDNA was generated using iScript Reverse Transcriptase kit (Bio-Rad, Hercules, CA). Quantitative real-time RT-PCR was performed using iQ SYBR Green Supermix and CFX96 real-time detection system (Bio-

Rad). β-actin was used as a normalizing control in all experiments. Real-time RT-PCR was performed equally by Michael Chang and Alex Panaccione.

Western blot analysis

To assess protein expression, western blot experiments were performed with the following antibodies: SOX10 (Abcam, ab155279), NOTCH1 (Cell Signaling, #3608), FABP7 (Cell Signaling, #13347), cleaved NOTCH1 (Cell Signaling, #4147), p27Kip1 (Cell Signaling, #2552), SKP2 (Cell Signaling, #4313), β-actin (Santa Cruz, sc-47778), and GAPDH (Santa Cruz, sc-25778). Pre-cast gels and Rapid Turbo-blot System protein transferring equipment were purchased from Bio-Rad. Gels were imaged and quantified using Molecular Imager Gel Doc XR+ System with Image Lab software (Bio-Rad). Western blot analysis was performed equally by Michael Chang and Alex Panaccione.

Immunofluorescence Staining

Cells were plated onto 8-well glass slides at a density of 25,000-30,000 cells per well, incubated for 24 h, washed twice with PBS, and fixed with 3-4% paraformaldehyde at room temperature (RT) for 30 minutes. Cell were permeabilized with 0.15% Triton X-100 in PBS for 5 minutes, washed twice, and blocked with 3% bovine serum albumin (BSA) for 30 minutes. Incubation with primary antibodies diluted in 3% BSA was performed at 4^{o}C overnight with subsequent washing once with PBS and once with 3% BSA. The following antibodies were used: SOX10 (Abcam, ab155279), FABP7 (Cell Signaling, D8N3N), NOTCH1 (Cell Signaling, D1E11), SKP2 (Cell Signaling #4313), JAG1 (Santa Cruz, C-20), NR2F1 (Santa Cruz, sc-74561) NR2F2 (Parsons Proteomics,

H7147), and AlexaFluor secondary antibodies (Life Tech). Slides were imaged by confocal microscopy. Immunofluorescence experiments were performed equally by Michael Chang, Alex Panaccione, and Bea Carbone.

CSC Isolation

For separation of $CD133^+$ and $CD133^-$ cells from bulk cultured cells or digested PDX tissue, cells were collected by trypsinization, rinsed in PBS, and filtered through a 100 uM cell strainer to obtain a single cell suspension. Cells were labelled with CD133-PE antibodies (Miltenyi, San Diego, CA) followed by CD133 Tumor Tissue MicroBead Kit (Miltenyi). Tumor cells underwent magnetic-activated cell sorting (MACS) by running through magnetic bead columns provided by Miltenyi. $CD133^+$ and $CD133^-$ cells were collected in separate tubes, and CD133 expression for each was verified using real time RT-PCR. Based on our experience, MACS is faster and more efficient in sorting large cell numbers compared to flow cytometry-based sorting methods, and was overall less harmful to live ACC cells than flow cytometry. CSC isolation was performed equally by Michael Chang and Alex Panaccione.

Tumorigenicity Assays

All mouse experiments were performed in accordance with NIH national guidelines and were approved by Yale Institutional Animal Care and Use Committee. Athymic *nu*/*nu* mice were purchased from NCI-Frederick (Frederick, MD). Mice were injected in the flanks subcutaneously with a specified number of viable tumor cells and measured weekly for tumor growth. Injected cells were either $CD133^+$, $CD133^-$, or bulk

tumor cells. Mice were sacrificed at a tumor volume of 1 cm^3 or if complications from tumor burden developed. Statistical analysis for significant differences tumor growth was performed using the two-tailed t-test. Tumorigenicity assays were performed equally by Michael Chang and Alex Panaccione.

Immunohistochemical Staining

Tumor tissue was sectioned, fixed, and analyzed by IHC staining using the following antibodies: cleaved NOTCH1 (Cell Signaling, Val1744), SOX10 (Cell Marque), and FABP7 (Abcam, Ab32423). IHC staining was performed by Yale Tissue Services.

Flow Cytometry

To assess effects of RNA knockdowns or DAPT treatment, cells either underwent DAPT versus DMSO treatment or transfection with siRNA against SOX10, NOTCH1, and FABP7 versus a control siRNA using lipofectamine in DMEM media. After 48-72 hours, cells were collected and incubated with CD133-PE antibody (Miltenyi) for 10 minutes. Fluorescence-activated cell sorting (FACS) was performed to determine percentage of $CD133^+$ cells using a FACS Caliber BD machine. Data analysis performed using Flowing Software version 2.5.0. Flow cytometry was performed equally by Michael Chang and Alex Panaccione.

Spheroidogenesis Assay

Cells were seeded in 6-well plates at approximately 50% confluency. Cells were treated with 1 or 10 μM gamma-secretase inhibitor DAPT (synonyms GSI-IX, LY-374973) from MedChem Express (Monmouth Junction, NJ) versus DMSO control, or using siRNA against NOTCH1, SOX10, and FABP7. At 24-hour intervals, 3 separate representative digital images per well at 4X magnification were used to quantify spheroid number. Statistical analysis was performed using a two-tailed t-test. Spheroidogenesis assays were performed by Michael Chang.

Spheroid Depletion Assay

Cells were seeded in 6-well plates at near-full confluency to allow for spheroid formation. After growth for 48 hours, cells were treated with varying concentrations of DAPT versus DMSO control. At 72 hour intervals, 3 separate representative digital images per well at 4X magnification were used to quantify spheroid number. Statistical analysis was performed using a two-tailed t-test. Spheroid depletion assays were performed by Michael Chang.

Cell Proliferation Assay

Cells were cultured in 96-well black clear bottom plates and treated with DAPT versus DMSO control. After cells were grown for 24-96 hours, viable cells were assessed by DNA quantification using the Cell Titer Glo system (Promega). Statistical analysis was performed using a two-tailed student t-test. Proliferation assays were performed by Michael Chang.

Cell Cycle Analysis

After treatment with DAPT versus DMSO control or siRNA against SOX10 and NOTCH1, cells were slowly fixed in 70% cold ethanol and stained with propidium iodide (PI). A Fluorescence-activated cell sorting (FACS) Caliber BD machine was used to analyze cells. Data analysis was performed using Flowing Software version 2.5.0. Cell cycle experiments were performed equally by Michael Chang and Alex Panaccione.

Cell Death Assay

After treatment with DAPT for >72 hours, cells were incubated for 10 minutes with CD133-FITC antibody (Miltenyi) as well as Annexin V antibody and 7-AAD DNA stain (Annexin V:PE apoptosis detection kit I, BD Biosciences). A FACS Caliber BD platform was used and data analysis was performed using Flowing Software version 2.5.0. Cell death assays were performed equally by Alex Panaccione and Michael Chang.

Radiation Sensitivity Assay

Cells were plated in T-25 flasks and irradiated with 3 or 6 Gy using Mark I Cesium-137 irradiator followed by 48 hours of incubation in the presence or absence of DAPT. Following treatment, cells were stained with CD133-PE antibody. FACS was performed to determine percentage of CD133+ cells. Radiosensitivity assays were performed in triplicate with statistical analysis by a two-tailed student t-test. Radiation sensitivity experiments were performed equally by Alex Panaccione and Michael Chang.

In Vivo Testing of DAPT Treatment

In vivo efficacy of DAPT (SelleckChem, Houston, TX) was evaluated in an Accx11 xenograft model generated via subcutaneous injection of 10^6 cultured Accx11 cells. Tumor cell-injected mice were randomized into control (vehicle-injected, N=5) and experimental (DAPT in corn oil, N=5) groups 15 days after cell injection. DAPT was administered intraperitoneally at 50 mg/kg, following an injection schedule of 3 days of treatment/4 days rest for 35 days. To assess DAPT toxicity, animals were observed daily and weighed weekly using a digital scale; data including individual and mean gram weights, mean percent weight change versus Day 0 and mean percent weight change versus prior measurement were recorded for each group and plotted at study completion. To assess DAPT efficacy, tumor dimensions were measured twice weekly by a digital caliper, and data including individual and mean estimated tumor volumes recorded for each group. Tumor volume (TV) was calculated using the formula $TV=width^2 \times length \times 0.52$. Statistical differences in tumor volume were determined using a two-tailed *t*-test. *In vivo* testing was performed by Alex Panaccione. Tumor processing was performed by Alex Panaccione and Michael Chang.

RESULTS

Generation and validation of cell cultures from ACC tissue

After the discovery that existing ACC cell lines were either contaminated or misidentified (61), the generation of new validated ACC cell lines is much needed to advance studies of this cancer. The rare incidence of ACC, however, limits the amount of clinical material available for culturing. To overcome this scarcity, we primarily used

tissue derived from previously verified PDX tumors (65) to generate new ACC cell lines. Through optimization of a recently published epithelial cell culturing protocol (109), we successfully generated intermediate- and long-term cell cultures from five ACC xenografts and one primary ACC tumor, Acc33 (Table 1). Successful cultures were derived from tumors with a diverse range of grades and histology. All six cultures proliferated for at least eight passages, with Accx11 and Acc33 reliably proliferating beyond 30 passages.

Cultures were primarily comprised of adherent spindle-shaped epithelial cells (Figure 1A). Of note, our most robust culture, Accx11, contained loosely adherent spheroid aggregates reminiscent of stem cells (Figure 1A, Accx11). All cultures yielded an adequate amount cells ($>10^6$) for molecular studies and cryopreservation.

To confirm the authenticity of newly created cell cultures, microsatellite profiling of eight sites was confirmed to match parental tumors (Table 2). Microsatellite profiles between culture and PDX tumors were near identical, with an acceptably small amount of drift as expected in culture environments. Cross-referencing these microsatellite profiles with those on publically available databases confirmed that these cell cultures were unique.

Cultured cells express markers specific to ACC

Previously identified ACC markers were used to validate the identity of cultured cells. Expression of TrkC/NTRK3, SOX10, NOTCH1, and FABP7 were found nearly universally in clinical ACC specimens and linked to an ACC-intrinsic gene signature that contained ~200 genes (51, 52, 110). Reassuringly, real time RT-PCR found that all ACC

cell cultures expressed high levels all four genes that was higher than levels in normal salivary gland (NSG) tissue with the exception of NOTCH1 expression in Accx2, Accx19, and Accx29 (Figure 1B). SOX10, NOTCH1, and FABP7 were similarly found to be highly expressed in PDX tumors (Supplemental Figure 1). Combining microsatellite and marker expression verification, these data demonstrate that a ROCK inhibitor- and cell feeder-based protocol is an effective solution to the ACC cell culture problem, and that these techniques can be used to advance translational ACC research.

ACC contains CD133+ spheroids that co-express SOX10, FABP7, NOTCH1, NOTCH1 targets, and neural stem cell markers

SOX10, a key neural stem cell marker, has been identified as signature of stem cells in cancers originating from neural crest. The SOX10 co-expression profile identified in ACC (51) suggested existence in ACC of cells with CSC properties. To validate this hypothesis, we profiled ACC for expression of cell surface markers that could be used for CSC isolation. Real time RT-PCR revealed that CD133/PROM1 (CD133), a cell surface marker of neural CSC (111), is expressed in all ACC cultures (Figure 1B) and ACC xenografts (Supplemental Figure 1).

To better characterize CD133-expressing ACC cells, a robustly proliferating and spheroid-forming culture, Accx11 was further investigated. FACS analysis of multiple passages showed that 2-15% of cultured cells expressed CD133 ($CD133^+$) (Supplemental Figure 2). Magnetic-activated cell sorting (MACS) separation of cultured Accx11 cells separated $CD133^+$ and $CD133^-$ subpopulations as indicated by more than a 50-fold enrichment of CD133 expression (Figure 2A). Notably, $CD133^+$ cells expressed at least

25-fold higher levels of SOX10, NOTCH1, and FABP7 compared to $CD133^-$ cells suggesting that expression of these genes co-segregated with cell surface expression of CD133 (Figure 2B).

After separation, cultured $CD133^+$ cells generated both spheroid-forming and tightly adherent cells, while cultured $CD133^-$ cells remained adherent and were not able to produce $CD133^+$ cells or spheroids (data not shown). These data suggest that $CD133^+$, but not $CD133^-$ cells, can reform both cell populations; however contamination of $CD133^+$ cells with $CD133^-$ cells remained a possibility. To further explore stem properties of $CD133^+$ cells, we investigated the expression of SCRG1, PLP1, MIA, SHC4, and TTYH1 that are components of the SOX10 co-expressed neural gene signature in ACC (51). Remarkably and without exception, these genes were more highly expressed in $CD133^+$ ACC cells compared to $CD133^-$ cells (Figure 2B). Given the association of these genes with stem cells of neurologic cancers (112-115), their selective expression in $CD133^+$ ACC provide additional support that ACC cultures contain neural stem-like cells (NSC).

Activation of Notch is a common feature of NSC and CSC (116) and Notch activation can be determined by levels of the intracellular domain (N1ICD). Western blot analysis revealed high expression of NOTCH1 and N1ICD in $CD133^+$ compared with $CD133^-$ or unsorted Accx11 cells and confirmed high expression levels of SOX10 and FABP7 in $CD133^+$ cells (Figure 2C). N1ICD is a marker of NOTCH1 activation as supported by increased expression of NOTCH canonical downstream targets HEY1, HEY2, and MYC in $CD133^+$ cells (Figure 2D).

To determine if other ACC cultures harbored similar cell populations, cultured cells derived from an independent xenograft were examined. FACS analyses of Accx19 cells found that 1-8% of total cells were $CD133^+$ (data not shown). MACS separation of Accx19 cells produced approximately a 3-fold enrichment of CD133 expression in $CD133^+$ cells compared to $CD133^-$ cells. In $CD133^+$ Accx19 cells, expression of NOTCH1, SOX10, and FABP7 was similarly enriched (Supplemental Figure 3A). Overall, these data supported the existence of a previously unknown population of cells in ACC that express both CD133 and SOX10 and contain activated NOTCH1.

$CD133^-$ ACC cells express neuronal differentiation markers NR2F1, NR2F2, p27Kip1, and Notch ligand JAG1

ACC cells expressing CD133 expressed markers typically found in undifferentiated neural lineage, including NOTCH1 and SOX10. Since cells lacking CD133 expression expressed much lower levels of markers of stemness, expression of neural differentiation markers was determined. NR2F1 and NR2F2, two orphan nuclear receptors important in mediating NSC differentiation (117), were expressed at markedly higher levels in $CD133^-$ ACC cells compared to $CD133^+$ cells (Figure 2E), suggesting that ACC cells lacking CD133 expression represent a more differentiated cell population. Finding neural differentiation markers in $CD133^-$ cells suggests that these more differentiated cells may have arisen from $CD133^+$ ACC cells that express markers of neural stemness.

JAG1, a canonical Notch ligand, is an activator of Notch signaling, and in many cancers it is expressed not in stem cells but in supporting niches (118, 119). Interestingly,

JAG1 expression was markedly higher (~11-fold) in Accx11 $CD133^-$ cells (Figure 2E). Similarly, NR2F2 and JAG1 were also expressed predominantly in $CD133^-$ cells isolated from Accx19 cultures (Supplemental Figure 3B).

$p27^{Kip1}$ is a cyclin-dependent kinase inhibitor that results in proliferative arrest and is a critical effector of neural differentiation whose expression is inhibited by activated NOTCH1 in NSC (120, 121). Given that in Accx11 cells NOTCH1 is preferentially activated in $CD133^+$ cells (Figure 2C) and that $CD133^-$ cells express markers of neural differentiation (Figure 2E), expression of p27Kip1 was measured in both ACC populations. Immunoblotting of unsorted and $CD133^-$ Accx11 cells after sorting revealed significantly higher p27Kip1 levels compared to the $CD133^+$ population (Figure 2F).

Immunofluorescence analysis confirms unique molecular profiles of $CD133^+$ and $CD133^-$ cells and supports NOTCH1/JAG1 interaction

RNA and protein expression analysis suggest that two previously unknown and distinct subpopulations within ACC can be reliably identified using a series of molecular markers. Based on selective expression of NOTCH1 and its targets in $CD133^+$ cells and JAG1 in $CD133^-$ cells, a model of inter-population signaling via NOTCH1/JAG1 interaction is proposed (Figure 2G). Immunofluorescence staining of cultured Accx11 cells supported this hypothesis with NOTCH1, SOX10, FABP7, and cell surface CD133 staining detected in a distinct cell population associated with less firmly attached cells, or spheroids, and NR2F1, NR2F2, and JAG1 detected in adherent cells. CD133 immunofluorescent staining was detected on a minority of cells within loosely adherent

cells that stained uniformly with NOTCH1 antibody, while the differentiation marker NR2F1 was detected only in the cytoplasm of adherent and more fusiform cells (Figure 2H and 2I). Differentiation markers NR2F1 (cytoplasmic) or NR2F2 (nuclear) were present in the attached cell population, but below the level of detection in less adherent spheroids (Figure 2I, 2J, and 2K). Remarkably, NOTCH1-expressing cells within spheroids were closely surrounded by adherent cells expressing membrane-localized JAG1 (Figure 2L). Z stack images revealed that JAG1 and NOTCH1 were co-localized on adjacent surfaces of cells within adherent and spheroid cells, respectively (Figure 2L, see arrows). Combined, these data support the existence of two cell subpopulations in ACC, one being more stem-like with expression of SOX10 and NOTCH1 and one being more differentiated. A co-dependence of these cell populations is possible given the expression of JAG1 on more differentiated $CD133^-$ ACC cells and its receptor, NOTCH1, on $CD133^+$ stem-like cells.

$CD133^+$ and $CD133^-$ populations identified in grafted ACC tissue

To determine if subpopulations of differentiated and stem-like cells exist more generally in ACC and to validate *in vitro* findings, CD133 expression was determined in a series of ACC patient-derived xenografts and markers of stemness and differentiation correlated. After dissociation and MACS sorting of five ACC PDX tumors, cell counting of viable cells found CD133 expression in 21 to 65% of cells (Figure 3A). Real-time PCR revealed that $CD133^+$ cells generally expressed higher levels of SOX10, NOTCH1, and FABP7 (Figure 3B, 3C, 3D, 3E). $CD133^-$ cells universally expressed higher levels of JAG1 with more variable expression level of NR2F1 (Figure 3F and 3G). These results

mirrored our findings in cultured cells, confirming the existence of two cell populations in ACC defined by expression phenotypes, $SOX10^{+}/NOTCH1^{+}/FABP7^{+}/CD133^{+}$ and $JAG1^{+}/NR2F1^{+}/ CD133^{-}$.

Tumorigenicity of ACC subpopulations

The ability of cultured ACC cells to initiate tumors was investigated via subcutaneous injections of 10^{6} cells into shoulder flanks of nude mice. Among ACC cultures tested to date, only Accx11 cells were tumorigenic in nude mice, forming tumors with solid histology and an intervening stromal component histologically similar to the parental patient tumor and PDX (Figure 4A). Relative expression of CD133, SOX10, NOTCH1, and FABP7 was similar in the original PDX and in the tumor produced from injection of cultured cells and higher than NSG as measured by RT-PCR and confirmed in tumor tissue by immunoblotting (Figure 4B and 4C).

In various cancer types, CD133 expression defines populations of CSC with enhanced tumor-initiating properties (122). To investigate CSC properties of CD133-expressing ACC cells, bulk Accx11 tumor cells were separated based on CD133 expression by MACS and 10^{4} cells were injected subcutaneously into right ($CD133^{+}$) and left ($CD133^{-}$) flanks of three nude mice. After 22 weeks, tumors were observed in 3 of 3 sites injected with $CD133^{+}$ cells, but in none of 3 sites injected with $CD133^{-}$ cells. At 32 weeks, a single tumor formed at a site injected with $CD133^{-}$ cells. Histologic evaluation of the parental ACCX11 tumor, tumors derived from $CD133^{+}$ cell injections, and the single tumor from a $CD133^{-}$ cell injection revealed similar histologic appearance (Supplemental Figure 4A). Expression analyses of CD133, SOX10, NOTCH1, and

FABP7 by real-time PCR and immunoblotting revealed expression of all markers in tumors derived from both $CD133^+$ and $CD133^-$ cells (Supplemental Figure 4B and 4C) suggesting that injected $CD133^-$ populations can convert to $CD133^+$ populations, or that separation of $CD133^+$ and $CD133^-$ cells was incomplete.

As experience with CD133 cell separation increased, we found that a single round of separation using CD133 antibody conjugated to beads left detectable traces of $CD133^+$ cells in the $CD133^-$ population, reflecting technical limitations of this procedure. Also, separation decreased viability of $CD133^+$ cells more than $CD133^-$ cells, possibly due to the damage inflicted by mechanical elution of column-bound cells (data not shown). To more adequately compare tumorigenicity of $CD133^+$ and $CD133^-$ cells, a second round of magnetic separation was performed on the unbound cells to isolate a more pure $CD133^-$ population. Following this double separation, 10^5 viable cells of each population were injected into the flanks of nude mice. Tumors began to form at the sites of $CD133^+$ injections as early as 6.5 weeks after injection. By 13 weeks post-injection, 4 of 5 $CD133^+$ injection sites had distinct tumors while none of 5 $CD133^-$ injections showed signs of tumor formation. Mean tumor volumes at 13 weeks were 0.14 cm^3 for tumors derived from $CD133^+$ and 0.01 cm^3 for tumors derived from $CD133^-$ cells (Figure 4D) ($p<0.05$). With a marked delay, 2 of 5 injection sites of $CD133^-$ cell injections formed small tumors with the earliest tumor developing at 19 weeks. At 27.5 weeks, 5 of 5 $CD133^+$ injection sites formed tumors, while no additional tumors grew in $CD133^-$ injection sites. Overall, these experiments demonstrated enhanced tumorigenicity of $CD133^+$ cells compared to $CD133^-$ cells.

Interdependence between NOTCH1, SOX10, and their common effector FABP7

Essential individual roles for SOX10 and NOTCH1 in NSC maintenance are well established, and loss of Notch signaling decreases SOX10 expression in neural progenitors (123, 124). FABP7 has recently been described as critical for proliferation and prevention of differentiation in neural progenitors (125) and as a marker of aggressive clinical behavior in ACC (52). Given that SOX10, NOTCH1, and FABP7 are each implicated in neural stemness, their interdependence in ACC cells was studied. Following individual knockdowns, expression of all three genes was measured by RT-PCR and immunoblotting. Depletion of SOX10 markedly decreased NOTCH1 expression and, reciprocally, knockdown of NOTCH1 was associated with decreased SOX10 both at the RNA and protein levels (Figure 5A and 5B). As expected, since FABP7 is a common target of NOTCH1 and SOX10 (56, 126), depletion of either NOTCH1 or SOX10 markedly suppressed FABP7 RNA and protein levels. Interestingly, knockdown of FABP7 also had suppressive effects on RNA levels of NOTCH1 and SOX10. At the protein level, FABP7 had no obvious effect on NOTCH1 expression while modestly decreasing SOX10 levels (Figure 5A and 5B). These data suggest the interdependence and potential functional cooperation of SOX10, NOTCH, and FABP7.

Although individual roles of NOTCH1 and SOX10 in CSC and NSC survival are well established, their roles in ACC, as well as co-operation via FABP7 and possibly other effectors has not yet been studied. To begin exploring the role of FABP7 in ACC signaling, gene expression profiling was performed in Accx11 cells following FABP7 depletion. Analyses revealed that 1158 genes were downregulated, and KEGG pathway analysis (http://bioinfo.vanderbilt.edu/webgestalt/) implicated these genes in cell cycle

regulation, ribosome biogenesis, cell metabolism, and signaling pathways regulating these processes (Table 3). Among these genes, 11 belonged to the Notch signaling network and 26 genes overlapped with the ACC SOX10 gene signature that we previously characterized (51). This observation further supported the feedback signaling from FABP7 to NOTCH1 and SOX10. In addition, SKP2, a major NOTCH1 effector involved in the regulation of cell cycle and proliferation (127), was among 31 cell cycle progression and 11 NOTCH1-regulated genes downregulated by FABP7 knockdown. In summary, these data suggested that NOTCH1, SOX10, and FABP7 may be co-regulated in ACC, and that FABP7 may serve as a pro-survival NOTCH1 and SOX10 effector.

SOX10, NOTCH1, and FABP7 are required for spheroidogenesis

NSC and CSC have the propensity to form spheroids in culture (128). Using spheroid formation as a surrogate of stem cell survival and proliferation, functional consequences of SOX10, NOTCH1, and FABP7 knockdowns were determined. Individual depletion of these genes significantly suppressed spheroid formation in cultured Accx11 cells (Figure 5C and 5D). These data suggested that SOX10, NOTCH1, and FABP7 are vital for spheroid formation, which could be due to a role in CSC survival and growth. Flow cytometry analysis of Accx11 was performed to assess the effects of SOX10, NOTCH1, and FABP7 depletion on cell cycle progression and cell survival. A marked (~4-6-fold) increase in the sub-G1 populations, indicating cell death, was observed following NOTCH1, SOX10, or FABP7 depletion (Figure 5E). Taken together, these results suggested that NOTCH1, SOX10, and FABP7 are important for survival of ACC cells, cell cycle progression, and maintenance of the stem-like subpopulation.

NOTCH1 depletion and gamma-secretase inhibition decrease CD133$^+$ cells

To test whether NOTCH1 is required for CD133$^+$ survival, the percentage of CD133$^+$ cells was measured following NOTCH1 knockdown in bulk Accx11 cells. NOTCH1 depletion resulted in a ~2.5-fold decrease in the proportion of CD133$^+$ cells (Figure 6A). Pharmacologic inhibitors of SOX10 and FABP7 are not available for clinical use at this time, however Notch signaling inhibitors are available in the form of gamma-secretase inhibitors that have advanced to clinical trials (129). Bulk Accx11 cells treated with gamma-secretase inhibitor, DAPT, suppressed spheroid formation in a concentration-dependent manner (Figure 6B and 6C). To determine if Notch signaling was also required for maintenance of pre-formed spheroids, Accx11 was grown to confluency to allow spheroid formation. Over a 9-day time course, a dose-dependent loss of pre-formed spheroids was observed in DAPT-treated Accx11 cells compared to controls (Figure 6D); however, the effect of gamma-secretase inhibition on maintenance of preformed spheroids was not as dramatic as its effect on spheroidogenesis and plateaued after six days.

To determine if DAPT activity was selective for CD133$^+$ cells, ACC cells were separated by MACS then treated with DAPT for 72 hours. DAPT treatment suppressed proliferation of CD133$^+$ cells with significant differences noted at all doses (1, 5, and 10μm), while proliferation of CD133$^-$ cells was not affected (Figure 6E). FACS analysis confirmed a selective DAPT effect, demonstrating a ~2.5-fold increase in sub-G1 population in CD133$^+$ cells without altering cell cycle progression in CD133$^-$ cells (Figure 5F), suggestive of selective cell death in the CD133$^+$ population. Annexin and 7-AAD co-staining confirmed that DAPT treatment selectively killed CD133$^+$ cells.

(Supplemental Figure 5). Interestingly, the pattern of cell death differed from that seen in apoptosis, suggesting an alternative cell death pathway induced by DAPT. Taken together, these data suggest that Notch signaling is critical in the proliferation and survival of CSC in ACC.

Notch signaling inhibitors prevent ACC tumor growth in mice

To perform a preclinical assessment of DAPT as a single agent treatment in ACC, Accx11 cells were injected subcutaneously into nude mice followed by 35-day treatment of peritoneally administered DAPT versus a vehicle control. In this study, DAPT had a statistically significant tumor-suppressive effect starting at two weeks (Figure 6G) without obvious signs of toxicity or loss of mouse weight. Overall, these *in vitro* and *in vivo* data suggest that Notch inhibitors could be advanced to clinical studies as a single-agent therapy for ACC.

Notch inhibition increases radiation sensitivity of CD133$^+$ cells

Because CSC are implicated in radiation resistance in many tumor types (122), the effect of targeting CD133$^+$ cells through Notch inhibition in combination with radiation was determined by treating cells with DAPT for 24 hours before irradiation. Radiation alone had minimal effect on the proportion of CD133$^+$ cells with 6 Gy of radiation decreasing this fraction only moderately, from 2.7 to 2.3%, (~15%) (Figure 6H). However, DAPT as a single agent showed a two-fold (~56%) decrease in the proportion of CD133$^+$ cells. Remarkably, when a single 3 Gy or 6 Gy dose of radiation was added to DAPT treatment, the combined effect resulted in an almost 2-fold

enhancement of $CD133^+$ cell depletion as compared with DAPT alone. DAPT induced statistically significant ($p<0.05$) depletion of $CD133^+$ levels at each dose of radiation when compared to radiation alone. The enhanced loss of $CD133^+$ ACC cells following radiation in the presence of DAPT suggest that Notch inhibitors may have a role in sensitization of ACC cells to radiation.

NOTCH1 depletion down-regulates SKP2, an E3 ubiquitin ligase that controls $p27^{Kip1}$

Activated NOTCH1 reduces $p27^{Kip1}$ levels by stimulating expression of the $p27^{Kip1}$ E3 ubiquitin-ligase, SKP2 (130). Identification of SKP2 downstream from a NOTCH1 effector, FABP7, suggested that SKP2 and $p27^{Kip1}$ may be engaged in the survival and proliferative NOTCH1 signaling in stem-like ACC cells. Indeed, we observed decreased expression of $p27^{Kip1}$ in $CD133^+$ Accx11 cells, where NOTCH1 was activated (Figure 2C and 2F). Assessment of SKP2 expression by RT-PCR and immunoblotting showed enrichment of SKP2 in $CD133^+$ compared to $CD133^-$ cells (Figure 7A and 7B). Immunofluorescent staining of Accx11 cultures revealed that SKP2 was detected primarily in NR2F1-negative spheroidal cells, and was localized within the cytoplasm (Figure 7C), where it has been associated with oncogenic activity (131). Since SKP2 is a NOTCH1 transcriptional target, inhibition of NOTCH1 activity is expected to suppress SKP2 expression and, in turn, increase $p27^{Kip1}$ protein stability and levels. In agreement with these expectations, siRNA-mediated NOTCH1 knockdown dramatically decreased SKP2 mRNA levels in Accx11 cells, as did DAPT treatment in a dose-dependent manner (Figure 7D and 7E). To determine if Notch effects on SKP2 and

$p27^{Kip1}$ are $CD133^+$-selective, bulk Accx11 cells, $CD133^+$, and $CD133^-$ populations were treated with DAPT for 48 hours then cell lysates subjected to immunoblot analysis. As expected, $CD133^+$ cells expressed higher levels of N1ICD than bulk or $CD133^-$ cells, and DAPT effectively inhibited NOTCH1 activation as marked by decreased N1ICD in these cells (Figure 7F). SKP2 was readily detected in only $CD133^+$ cells, whereas $p27^{Kip1}$ was detected in $CD133^-$ cells at much higher levels than in $CD133^+$ cells. Treatment with DAPT did not markedly alter expression of $p27^{Kip1}$ in bulk or $CD133^-$ cells, but dramatically enhanced its expression in $CD133^+$ cells (Figure 7F). Together, these data suggest a possible mechanism by which NOTCH1 inhibition decreases oncogenic activity in ACC is through downregulation of SKP2 and upregulation $p27^{Kip1}$ selectively in $CD133^+$ cells.

DISCUSSION

The significance of these studies lies partially in their ability to provide a framework and tools to begin addressing many of the current difficulties in ACC research. Advancements at both the basic science and clinical level include creation of validated cell cultures lacking widespread contamination previously observed in ACC cell lines (61) and providing a platform for pre-clinical studies to avoid continued high failure rates of clinical trials for systemic therapies in ACC (32). We demonstrate a new and effective method for culturing ACC cells from PDX and patient tumors, enabling functional experimentation and in-depth study of ACC biological drivers.

While CD133 expression was recently reported in ACC (132), there have been no published attempts to isolate and characterize $CD133^+$ ACC cells. Techniques described

here were used to isolate an enriched $CD133^+$ population and characterize gene expression within this ACC subpopulation. Expression of SOX10, NOTCH1, FABP7, and multiple key neural stem cell regulators along with their potent tumor-initiating activity suggest that $CD133^+$ expression marks a neural stem-like population of cells within ACC. Furthermore, we demonstrate a role of SOX10, NOTCH1, and FABP7 for proliferation and radiation resistance of $CD133^+$ cells, identifying new potential pathways to target in ACC treatment. It will be interesting to determine if other molecular defects in ACC, including MYB fusions, are also involved in ACC stem cell survival or maintenance. Treatment for this cancer is in much need of a novel approach, and selective targeting of CSC may address issues of recurrence and relentless growth even after radiotherapy.

Gene knockdown studies highlighted the essential roles and potential functional cooperation between NOTCH1 and SOX10 in maintenance of $CD133^+$ ACC cells. An important and previously unappreciated insight into this cooperation was provided by the co-expression and interdependence of FABP7 with NOTCH1 and SOX10, as well as the role of FABP7 in regulating expression of genes critical for cell survival. FABP7 has been recently described as a novel diagnostic and prognostic ACC marker (52) and is also implicated in glioblastoma, melanoma, and basal-like breast cancer (53, 133, 134); however, its downstream targets and molecular mechanisms of activation have not been extensively studied. Data presented herein associated FABP7 with the expression of SKP2 and multiple other genes involved in survival, proliferation, and metabolic pathways identifying a novel signaling pathway that stimulates CSC in ACC. Importantly, these findings may extend beyond ACC to other cancers of neural origin in

which SOX10/NOTCH1/FABP7 signaling may also have crucial driving roles and therefore therapeutic relevance.

As multiple Notch inhibitors have recently entered clinical trials for ACC, the findings of our study support the rationale behind these investigations. We demonstrate that a gamma secretase inhibitor selectively triggers cells death in tumor-initiating cancer stem cells, suggesting that Notch inhibitors have potential therapeutic roles in monotherapy or as an adjunct to initial surgery to prevent recurrence. Additionally, we demonstrate that CSC in ACC are sensitized to radiation when treated with a gamma secretase inhibitor, suggesting that Notch inhibitors may also have a significant neoadjuvant or adjuvant treatment role with radiation.

Notch targeting with gamma-secretase inhibitors in trials for other cancers have been largely plagued by severe gastrointestinal side-effects attributed to the broad off-target effects of gamma secretase inhibition. This has prompted the development and clinical testing of more specific inhibitors of Notch signaling, which include monoclonal antibodies against specific Notch receptors such as tareztumab (anti-Notch2/3) and brontictuzumab (anti-Notch1) as well as antibodies against activating ligands of Notch such as demcizumab and OMP-305B83 (both anti-DLL4) (OncoMed). Brontictuzumab is one of the drugs currently under investigation in a phase I trial for ACC. Multiple other small molecule inhibitors of the Notch pathway are in preclinical development.

In this study we have also identified other potential therapeutic targets that can be the subject of future studies. Detection of JAG1 expression on the surface of $CD133^-$ ACC cells provides an important insight into evolutionary conserved molecular mechanisms of communication between $CD133^-$ and $CD133^+$ cells. Since JAG1

expression in cancer has been linked to angiogenesis, chemoresistance, and poor survival (118), JAG1 targeting may provide additional means for therapeutic interventions aimed at both CD133- and CD133+ cell populations.

Association of NOTCH1 activation with SKP2 and $p27^{Kip1}$ provided an interesting insight into CSC-specific signaling in ACC. In addition to its central roles in the regulation of proliferation, apoptosis, and senescence, which are mediated via $p27^{Kip1}$ (135), SKP2 is critically involved in tumor survival during energy stress (136, 137). SKP2 functions at a crossroad of many oncogenic signaling axes, suggesting that SKP2 inhibitors may increase efficacy of future CSC-targeting ACC therapies when used in combination with Notch inhibitors.

It is important to recognize the limitations of this study. Given the rarity and unpredictability of cancer, it is difficult to assess generalizability of our findings to all cases of ACC, as the majority of our *in vitro* investigations were performed in one or two cell lines, Accx11 and Accx19. However, our immunomagnetic sorting and expression analysis of all available patient-derived xenograft tumors suggest that $CD133^{+}$ cells expressing a similar expression profile are found in the majority of ACC specimens, and that all tested ACC tumors from patients expressed a neural stem gene expression pattern based on SOX10 (51). Future studies should aim to perform these experiments in other cell cultures and lines to determine the external validity of our findings. Additionally, while microsatellite analyses show little drift from xenograft to tumor, all cultures derived from PDX tumors may have already selected for the most robustly proliferating cells. While we did have success in establishing one culture directly from tumor tissue, these efforts will need to be continued in the future to ensure that cultured cells represent

clinical specimens as reliably as possible. In our treatment of ACC cells, we recognize that gamma-secretase inhibitors are known to have several off-target effects in addition to interference with Notch signaling. Observation of similar outcomes with depletion of NOTCH1 was reassuring that the biologic response to gamma secretase activity was mediated largely through NOTCH inhibition, but animal studies could not be performed with more specific NOTCH inhibition. Therefore, some assays may have been unknowingly altered by off-target effects of gamma secretase inhibition, and future studies are needed with more specific Notch inhibitors to clarify the precise role of Notch in $CD133^+$ cell maintenance and radiation resistance.

Overall, characterization of neural stem-like cells in ACC and delineating signaling events essential for their maintenance provide a new concept for ACC treatment that focuses on the clinical significance of cancer cells with neural stem properties. Continued study into the characteristics of this newly identified subpopulation of cells has the potential to open additional therapeutic opportunities for a relentless cancer that greatly needs new approaches.

REFERENCES

1. Robin C, Laboulbene A. Memoire sur trois productions morbides nondescrites. Soc Biol Mem. 1853;V:185-96.
2. Billroth T. Beobachtungen uber Geschwulste der Speicheldrüsen. Virchows Arch Pathol Anat. 1859;17:357-75.
3. Spies JW. Adenoid cystic carcinoma. Arch Surg. 1930;21:365-404.
4. Foote FW, Frazell EL. Tumours of the major salivary glands. Cancer. 1953;6:1065-133.
5. Conley J, Dingman DL. Adenoid cystic carcinoma of the head and neck (cylindroma). Arch Otolaryngol. 1974;100:81-90.
6. Fitzpatrick PJ, Theriault C. Malignant salivary gland tumors. Int J Radiat Oncol Biol Phys. 1986;12:1743-7.
7. Boukheris H, Curtis RE, Land CE, Dores GM. Incidence of carcinoma of the major salivary glands according to the WHO classification, 1992 to 2006. Oral Surg Oral Med Oral Pathol Oral Radiol Endod. 2009;91:194-9.
8. Yu T, Gao QH, Wang XY, Wen YM, Li LJ. Malignant sublingual gland tumors: a retrospec- tive clinicopathologic study of 28 cases. Oncology. 2007;72:39-44.
9. Hellquist H, Skalova A. Adenoid cystic carcinoma. Histopathology of the Salivary Glands. Berlin: Springer-Verlag; 2014. p. 221-60.
10. Ascani G, Pieramici T, Messi M, Lupi E, Rubini C, et al. Salivary gland tumours: a retro- spective study of 454 patients. Minerva Stomatol. 2006;55:209-14.
11. Bradley PJ. Adenoid cystic carcinoma of the head and neck: a review. Curr Opin Otolaryngol Head Neck Surg. 2004;12:127-32.
12. Bennett AK, Mills SE, Wick MR. Salivary- type neoplasms of the breast and lung. Semin Diagn Pathol. 2003;20:279-304.
13. Iczkowski KA, Ferguson KL, Grier DD, Hossain D, Banerjee SS, et al. Adenoid cystic/ basal cell carcinoma of the prostate: clinicopathologic findings in 19 cases. Am J Surg Pathol. 2003;27:1523-9.
14. Fueston JC, Gloster HM, Mutasim DF. Primary cutaneous adenoid cystic carcinoma: a case report and review of the literature. Cutis. 2006;77:157-60.
15. Elhassani LK, Mrabti H, Ismaili N, Bensouda Y, Masbah O, et al. Advanced adenoid cystic carcinoma of the cervix: a case report and review of the literature. Cases. 2009;2:6634.
16. Ellington CL, Goodman M, Kono SA, Grist W, Wadsworth T, et al. Adenoid cystic carcinoma of the head and neck. Cancer. 2012;118:4444-51.
17. Adenoid Cystic Carcinoma Research Foundation. Understanding ACC. Needham, MA2015 [cited 2015 December 22]. Available from: http://www.accrf.org/living-with-acc/understanding-acc/.
18. Spiro RH, Huvos AG, Strong EW. Adenoid cystic carcinoma of salivary origin. Am J Surg. 1974;128(4):512-20.
19. Min R, Siyi L, Wenjun Y, Ow A, Lizheng W, et al. Salivary gland adenoid cystic carcinoma with cervical lymph node metastasis: a preliminary study of 62 cases. Int J Oral Maxillofac Surg. 2012;41:952-7.
20. Bradley PJ. Distant metastases from salivary glands. Cancer. 2001;63:233-42.

21. Spiro RH. Distant metastases in adenoid cystic carcinoma of salivary origin. Am J Surg. 1997;174:495-8.
22. van der Wal JE, Becking AG, Snow GB, van der Waal I. Distant metastases of adenoid cystic carcinoma of the salivary glands and the value of diagnostic examinations during follow-up. Head Neck. 2002;24(8):779-83.
23. Nagel H, Hotze HJ, Laskawi R, Chilla R, Droese M. Cytologic diagnosis of adenoid cystic carcinoma of salivary glands. Diagn Cytopath. 1998;20(6):358-66.
24. Sigal R, Monnet R, de Baere T, Micheau C, Shapeero LG, et al. Adenoid cystic carcinoma of the head and neck: evaluation with MR imaging and clinical-pathologic correlation in 27 patients. Radiology. 1992;184(1):95-101.
25. Westra WH. The surgical pathology of salivary gland neoplasms. Otolaryngol Clin North Am. 1999;32(5):919-43.
26. Spiro RH, Huvos AG. Stage means more than grade in adenoid cystic carcinoma. Am J Surg. 1992;164:623-8.
27. Chen AM, Bucci MK, Weinberg V, Garcia J, Quivey JM, et al. Adenoid cystic carcinoma of the head and neck treated by surgery with or without postoperative radiation therapy: prognostic features of recurrence. Int J Radiat Oncol Biol Phys. 2006;66(1):152-9.
28. Darling MR, Schneider JW, Phillips VM. Polymorphous low-grade adenocarcinoma and adenoid cystic carcinoma: a review and comparison of immunohistochemical markers. Oral Oncol. 2002;38(7):641-5.
29. Garden AS, Weber RS, Morrison WH, Ang KK, Peters LJ. The influence of positive margins and nerve invasion in adenoid cystic carcinoma of the head and neck treated with surgery and radiation. Int J Radiat Oncol Biol Phys. 1995;32(3):619-25.
30. Silverman DA, Carlson TP, Khuntia D, Bergstrom RT, Saxton J, et al. Role for postoperative radiation therapy in adenoid cystic carcinoma of the head and neck. Laryngoscope. 2004;114(7):1194-9.
31. Meyers M, Granger B, Herman P, Janot F, Garrel R, et al. Head and neck adenoid cystic carcinoma: A prospective multicenter REFCOR study of 95 cases. Eur Ann Otorhinolaryngol Head Neck Dis. 2015:Epub ahead of print. Epub Oct 19.
32. Laurie SA, Ho AL, Fury MG, Sherman E, Pfister DG. Systemic therapy in the management of metastatic or locally recurrent adenoid cystic carcinoma of the salivary glands: a systematic review. Lancet. 2011;12:815-24.
33. Fordice J, Kershaw C, El-Naggar A, Goepfert H. Adenoid cystic carcinoma of the head and neck: predictors of morbidity and mortality. Arch Otolaryngol Head Neck Surg. 1999;125(2):149-52.
34. da Cruz Perez DE, de Abreu Alves F, Nobuko Nishimoto I, de Almeida OP, Kowalski LP. Prognostic factors in head and neck adenoid cystic carcinoma. Oral Oncol. 2006;42(2):139-46.
35. Stephens PJ, Davies HR, Mitani Y, Van Loo P, Shlien A, et al. Whole exome sequencing of adenoid cystic carcinoma. J Clin Invest. 2013;123(7):2965-8.
36. Ho AS, Kannan K, Roy DM, Morris LG, Ganly I, et al. The mutational landscape of adenoid cystic carcinoma. Nat Genet. 2013;45(7):791-8.
37. Frierson HF, Moskaluk CA. Mutation signature of adenoid cystic carcinoma: evidence for transcriptional and epigenetic reprogramming. J Clin Invest. 2013;123(7):2783-5.

38. Persson M, Andrén Y, Moskaluk CA, Frierson HF Jr, Cooke SL, et al. Clinically significant copy number alterations and complex rearrangements of MYB and NFIB in head and neck adenoid cystic carcinoma. Genes Chromosomes Cancer. 2012;51(8):805-17.
39. Mitani Y, Liu B, Rao P, Borra V, Zafereo M, et al. Novel MYBL1 gene rearrangements with recurrent MYBL1-NFIB fusions in salivary adenoid cystic carcinomas lacking t(6;9) translocations. Clin Cancer Res. 2015. Epub Dec 2 [Epub ahead of print].
40. Mitani Y, Li J, Rao PH, Zhao YJ, Bell D, et al. Comprehensive analysis of the MYB-NFIB gene fusion in salivary adenoid cystic carcinoma: Incidence, variability, and clinicopathologic significance. Clin Cancer Res. 2010;16(19):4722-31.
41. Engelman JA. Targeting PI3K signalling in cancer: opportunities, challenges and limitations. Nat Rev Cancer. 2009;9:550-62.
42. Frierson HF, El-Naggar AK, Welsh JB, Sapinoso LM, Su AI, et al. Large scale molecular analysis identifies genes with altered expression in salivary adenoid cystic carcinoma. Am J Pathol. 2002;161(4):1315-23.
43. Phuchareon J, van Zante A, Overdevest JB, McCormick F, Eisele DW, et al. c-Kit expression is rate-limiting for stem cell factor-mediated disease progression in adenoid cystic carcinoma of the salivary glands. Transl Oncol. 2014;7(5):537-45.
44. Lennartsson J, Ronnstrand L. Stem cell factor receptor/c-Kit: from basic science to clinical implications. Physiol Rev. 2012;92:1619-49.
45. Ratajczak MZ, Perrotti D, Melotti P, Powzaniuk M, Calabretta B, et al. Myb and ets proteins are candidate regulators of c-kit expression in human hematopoietic cells. Blood. 1998;91(6):1934-46.
46. Hirota S, Isozaki K, Moriyama Y, Hashimoto K, Nishida T, et al. Gain-of-function mutations of c-kit in human gastrointestinal stromal tumors. Science. 1998;279:577.
47. Kemmer K, Corless CL, Fletcher JA, McGreevey L, Haley A, et al. KIT mutations are common in testicular seminomas. Am J Pathol. 2004;164:305.
48. Demetri GD, von Mehren M, Blanke CD, Van den Abbeele AD, Eisenberg B, et al. Efficacy and safety of imatinib mesylate in advanced gastrointestinal stromal tumors. N Engl J Med. 2002;347(7):472-80.
49. Pfeffer MR, Talmi Y, Catane R, Symon Z, Yosepovitch A, et al. A phase II study of Imatinib for advanced adenoid cystic carcinoma of head and neck salivary glands. Oral Oncol. 2007;43(1):33-6.
50. Lin CH, Yen RF, Jeng YM, Tzen CY, Hsu C, et al. Unexpected rapid progression of metastatic adenoid cystic carcinoma during treatment with imatinib mesylate. Head Neck. 2005;27(12):1022-7.
51. Ivanov SV, Panaccione A, Nonaka D, Prasad ML, Boyd KL, et al. Diagnostic SOX10 gene signatures in salivary adenoid cystic and breast basal-like carcinomas. Br J Cancer. 2013;109(2):444-51.
52. Phuchareon J, Overdevest JB, McCormick F, Eisele DW, van Zante A, et al. Fatty acid binding protein 7 is a molecular marker in adenoid cystic carcinoma of the salivary glands: implications for clinical significance. Transl Oncol. 2014;7(6):780-7.

53. Liang Y, Bollen AW, Aldape KD, Gupta N. Nuclear FABP7 immunoreactivity is preferentially expressed in infiltrative glioma and is associated with poor prognosis in EGFR-overexpressing glioblastoma. BMC Cancer. 2006;6:97.
54. Alshareeda AT, Rakha EA, Nolan CC, Ellis IO, Green AR. Fatty acid binding protein 7 expression and its sub-cellular localization in breast cancer. Breast Canc Res Treat. 2012;134(2):519-29.
55. Yasumoto Y, Miyazaki H, Vaidyan LK, Kagawa Y, Ebrahimi M, et al. Inhibition of fatty acid synthase decreases expression of stemness markers in glioma stem cells. PLoS One. 2016;11(1):e0147717.
56. Anthony TE, Mason HA, Gridley T, Fishell G, Heintz N. Brain lipid-binding protein is a direct target of Notch signaling in radial glial cells. Genes Dev. 2005;19(9):1028-33.
57. Bell A, Bell D, Weber RS, El-Naggar AK. CpG island methylation profiling in human salivary gland adenoid cystic carcinoma. Cancer. 2011;117(13):2898-909.
58. Stoeck A, Lejnine S, Truong A, Pan L, Wang H, et al. Discovery of biomarkers predictive of GSI response in triple-negative breast cancer and adenoid cystic carcinoma. Cancer Discov. 2014;4(10):1154-67.
59. Ferrando AA. The role of NOTCH1 signaling in T-ALL. Hematology Am Soc Hematol Educ Program. 2009;2009:353-61.
60. Agrawal N, Frederick MJ, Pickering CR, Bettegowda C, Chang K, et al. Exome sequencing of head and neck squamous cell carcinoma reveals inactivating mutations in NOTCH1. Science. 2011;333:1154-7.
61. Phuchareon J, Ohta Y, Woo JM, Eisele DW, Tetsu O. Genetic profiling reveals cross-contamination and misidentification of 6 adenoid cystic carcinoma cell lines: ACC2, ACC3, ACCM, ACCNS, ACCS and CAC2. PLoS One. 2009;4(6):e6040.
62. Li SL. Establishment of a human cancer cell line from adenoid cystic carcinoma of the minor salivary gland. Zhonghua Kou Qiang Yi Xue Za Zhi. 1990;25(1):29-31.
63. Wang L, Wang Y, Bian H, Pu Y, Guo C. Molecular characteristics of homologous salivary adenoid cystic carcinoma cell lines with different lung metastasis ability. Oncol Rep. 2013;30:207.
64. Li J, Perlaky L, Rao P, Weber RS, El-Naggar AK. Development and characterization of salivary adenoid cystic carcinoma cell line. Oral Oncol. 2014;50(10):991-9.
65. Moskaluk CA, Baras AS, Mancuso SA, Fan H, Davidson RJ, et al. Development and characterization of xenograft model systems for adenoid cystic carcinoma. Lab Invest. 2011;91(10):1480-90.
66. van Herpen CM, Locati LD, Buter J, Thomas J, Bogaerts J, et al. Phase II study on gemcitabine in recurrent and/or metastatic adenoid cystic carcinoma of the head and neck. Eur J Cancer. 2008;44(17):2542-5.
67. Gilbert J, Li Y, Pinto HA, Jennings T, Kies MS, et al. Phase II trial of taxol in salivary gland malignancies (E1394): a trial of the Eastern Cooperative Oncology Group. Head Neck. 2006;28(3):197-204.
68. Schramm Jr VL, Srodes C, Myers EN. Cisplatin therapy for adenoid cystic carcinoma. Arch Otolaryngol. 1981;107(739-741).
69. Licitra L, Marchini S, Spinazzè S, Rossi A, Rocca A, et al. Cisplatin in advanced salivary gland carcinoma. A phase II study of 25 patients. Cancer. 1991;68(9):1874-7.

70. Mattox DE, Von Hoff DD, Balcerzak SP. Southwest Oncology Group study of mitoxantrone for treatment of patients with advanced adenoid cystic carcinoma of the head and neck. Invest New Drugs. 1990;8:105-7.
71. Verweij J, de Mulder PH, de Graeff A, Vermorken JB, Wildiers J, et al. Phase II study on mitoxantrone in adenoid cystic carcinomas of the head and neck. EORTC Head and Neck Cancer Cooperative Group. Ann Oncol. 1996;7(8):867-9.
72. Vermorken JB, Verweij J, de Mulder PH, Cognetti F, Clavel M, et al. Epirubicin in patients with advanced or recurrent adenoid cystic carcinoma of the head and neck: a phase II study of the EORTC Head and Neck Cancer Cooperative Group. Ann Oncol. 1993;4(9):785-8.
73. Airoldi M, Pedani F, Succo G, Gabriele AM, Ragona R, et al. Phase II randomized trial comparing vinorelbine versus vinorelbine plus cisplatin in patients with recurrent salivary gland malignancies. Cancer. 2001;91(3):541-7.
74. Dreyfuss AI, Clark JR, Fallon BG, Posner MR, Norris CM Jr, et al. Cyclophosphamide, doxorubicin, and cisplatin combination chemotherapy for advanced carcinomas of salivary gland origin. Cancer. 1987;2869-2872.
75. Belani CP, Eisenberger MA, Gray WC. Preliminary experience with chemotherapy in advanced salivary gland neoplasms. Med Pediatr Oncol. 1988;16:197-202.
76. Creagan ET, Woods JE, Rubin J, Schaid DJ. Cisplatin-based chemotherapy for neoplasms arising from salivary glands
and contiguous structures in the head and neck. Cancer. 1988;62:2313-9.
77. Licitra L, Cavina R, Grandi C, Palma SD, Guzzo M, et al. Cisplatin, doxorubicin and cyclophosphamide in advanced salivary gland carcinoma:
a phase II trial of 22 patients. Ann Oncol. 1996;7(6):640-2.
78. Hotte SJ, Winquist EW, Lamont E, MacKenzie M, Vokes E, et al. Imatinib mesylate in patients with adenoid cystic cancers of the salivary glands expressing c-kit: a Princess Margaret Hospital phase II consortium study. J Clin Oncol. 2005;23(3):585-90.
79. Guigay JM, Bidault F, Temam S, Janot F, Raymond E, et al. Antitumor activity of imatinib in progressive, highly expressing KIT adenoid cystic carcinoma of the salivary glands: a phase II study. Proc Am Soc Clin Oncol. 2007;25:6086.
80. Ochel HJ, Gademann G, Rocken C, Wordehoff H. Effects of imatinib mesylate on adenoid cystic carcinomas. Anticancer Res. 2005;25:3659-64.
81. Slevin NJ, Mais KL, Bruce I. Imatinib with cisplatin in recurrent and/or metastatic adenoidcystic carcinoma-preliminary results
of a phase II study of 18 patients with response assessed by morphological and functional imaging. Eur J Cancer. 2005;3:292-3.
82. Vered M, Braunstein E, Buchner A. Immunohistochemical study of epidermal growth factor receptor in adenoid cystic carcinoma of salivary gland origin. Head Neck. 2002;24:632-6.
83. Jakob JA, Kies MS, Glisson BS, Kupferman ME, Liu DD, et al. Phase II study of gefitinib in patients with advanced salivary gland cancers. Head Neck. 2015;37(5):644-9.
84. Agulnik M, Cohen EW, Cohen RB, Chen EX, Vokes EE, et al. Phase II study of lapatinib in recurrent or metastatic epidermal growth factor receptor and/or erbB2 expressing adenoid cystic carcinoma and non adenoid cystic carcinoma malignant tumors of the salivary glands. J Clin Oncol. 2007;25(25):3978-84.

85. Locati LD, Bossi P, Perrone F, Potepan P, Crippa F, et al. Cetuximab in recurrent and/or metastatic salivary gland carcinomas: A phase II study. Oral Oncol. 2009;45(7):574-8.
86. Hitre E, Budai B, Takácsi-Nagy Z, Rubovszky G, Tóth E, et al. Cetuximab and platinum-based chemoradio- or chemotherapy of patients with epidermal growth factor receptor expressing adenoid cystic carcinoma: a phase II trial. Br J Cancer. 2013;109(5):1117-22.
87. Keam B, Kim SB, Shin SH, Cho BC, Lee KW, et al. Phase 2 study of dovitinib in patients with metastatic or unresectable adenoid cystic carcinoma. Cancer. 2015;121(15):2612-7.
88. Chau NG, Hotte SJ, Chen EX, Chin SF, Turner S, et al. A phase II study of sunitinib in recurrent and/or metastatic adenoid cystic carcinoma (ACC) of the salivary glands: current progress and challenges in evaluating molecularly targeted agents in ACC. Ann Oncol. 2012;23(6):1562-70.
89. Argiris A, Ghebremichael M, Burtness B, Axelrod RS, Deconti RC, et al. A phase 2 trial of bortezomib followed by the addition of doxorubicin at progression in patients with recurrent or metastatic adenoid cystic carcinoma of the head and neck: a trial of the Eastern Cooperative Oncology Group (E1303). Cancer. 2011;117(15):3374-82.
90. Liu W, Huang S, Chen Z, Wang H, Wu H, et al. Temsirolimus, the mTOR inhibitor, induces autophagy in adenoid cystic carcinoma: in vitro and in vivo. Pathol Res Pract. 2014;210(11):764-9.
91. Kim DW, Oh DY, Shin SH, Kang JH, Cho BC, et al. A multicenter phase II study of everolimus in patients with progressive unresectable adenoid cystic carcinoma. BMC Cancer. 2014;14:795.
92. Adenoid Cystic Carcinoma Research Foundation. Selected Phase I Clinical Trials of NOTCH Inhibitors 2014 [updated May 2014; cited 2015 Dec 25]. Available from: http://www.accrf.org/wp-content/uploads/Clinical-Trials-Phase-I-2014-May.pdf.
93. Wicha MS, Liu S, Dontu G. Cancer stem cells: an old idea – a paradigm shift. Cancer Res. 2006;66:1883-90.
94. Lapidot T, Sirard C, Vormoor J, Murdoch B, Hoang T. A cell initiating human acute myeloid leukaemia after transplantation into SCID mice. Nature. 1994;367:645-8.
95. Prince ME, Sivanandan R, Kaczorowski A, Wolf GT, Kaplan MJ, et al. Identification of a subpopulation of cells with cancer stem cell properties in head and neck squamous cell carcinoma. Proc Natl Acad Sci U S A. 2007;104:973-8.
96. Vermeulen L, Todaro M, de Sousa Mello F, Sprick MR, Kemper K, et al. Single-cell cloning of colon cancer stem cells reveals a multi-lineage differentiation capacity. Proc Natl Acad Sci U S A. 2008;105:13427-32.
97. Li C, Lee CJ, Simeone DM. Identification of human pancreatic cancer stem cells. Methods Mol Biol. 2009;568:161-73.
98. Schiapparelli P, Enguita-Germán M, Balbuena J, Rey JA, Lázcoz P, et al. Analysis of stemness gene expression and CD133 abnormal methylation in neuroblastoma cell lines. Oncol Rep. 2010;24(5):1355-62.
99. Pearce DJ, Taussig D, Simpson C, Allen K, Rohatiner AZ, et al. Characterization of cells with a high aldehyde dehydrogenases activity from cord blood and acute myeloid leukemia samples. Stem Cells. 2005;23:752-60.

100. Huang EH, Hynes MJ, Zhang T, Ginestier C, Dontu G, et al. Aldehyde dehydrogenase 1 is a marker for normal and malignant human colonic stem cells (SC) and tracks SC overpopulation during colon tumorigenesis. Cancer Res. 2009;69(8):3382-9.
101. Sun S, Wang Z. ALDH high adenoid cystic carcinoma cells display cancer stem cell properties and are responsible for mediating metastasis. Biochem Biophys Res Commun. 2010;396(4):843-8.
102. Farnie G, Clarke RB. Mammary stem cells and breast cancer-role of Notch signalling. Stem Cell Rev. 2007;3:169-75.
103. Wang Z, Ahmad A, Li Y, Azmi AS, Miele L, et al. Targeting notch to eradicate pancreatic cancer stem cells for cancer therapy. Anticancer Res. 2011;31(4):1105-13.
104. Fan X, Matsui W, Khaki L, Stearns D, Chun J, et al. Notch pathway inhibition depletes stem-like cells and blocks engraftment in embryonal brain tumors. Cancer Res. 2006;66(15):7445-52.
105. Fan X, Khaki L, Zhu TS, Soules ME, Talsma CE, et al. NOTCH pathway blockade depletes CD133-positive glioblastoma cells and inhibits growth of tumor neurospheres and xenografts. Stem Cells. 2010;28(1):5-16.
106. Farnie G, Clarke RB, Spence K, Pinnock N, Brennan K, et al. Novel cell culture technique for primary ductal carcinoma in situ: role of Notch and epidermal growth factor receptor signaling pathways. J Natl Cancer Inst. 2007;99(8):616-27.
107. Wang J, Wakeman TP, Lathia JD, Hjelmeland AB, Wang XF, et al. Notch promotes radioresistance of glioma stem cells. Stem Cells. 2010;28(1):17-28.
108. Wang Z, Li Y, Kong D, Banerjee S, Ahmad A, et al. Acquisition of epithelial-mesenchymal transition phenotype of gemcitabine-resistant pancreatic cancer cells is linked with activation of the notch signaling pathway. Cancer Res. 2009;69(6):2400-7.
109. Liu X, Ory V, Chapman S, Yuan H, Albanese C, et al. ROCK inhibitor and feeder cells induce the conditional reprogramming of epithelial cells. Am J Pathol. 2012;180:599.
110. Ivanov SV, Panaccione A, Brown B, Guo Y, Moskaluk CA, et al. TrkC signaling is activated in adenoid cystic carcinoma and requires NT-3 to stimulate invasive behavior. Oncogene. 2013;32(32):3698-710.
111. Grosse-Gehling P, Fargeas CA, Dittfeld C, Garbe Y, Alison MR, et al. CD133 as a biomarker for putative cancer stem cells in solid tumours: limitations, problems and challenges. J Pathol. 2013;229(3):355-78.
112. Archer TC, Pomeroy SL. A developmental program drives aggressive embryonal brain tumors. Nat Genet. 2014;46(1):2-3.
113. Chen Z, Liu C, Patel AJ, Liao CP, Wang Y, et al. Cells of origin in the embryonic nerve roots for NF1-associated plexiform neurofibroma. Cancer Cell. 2014;26(5):695-706.
114. Fagiani E, Giardina G, Luzi L, Cesaroni M, Quarto M, et al. RaLP, a new member of the Src homology and collagen family, regulates cell migration and tumor growth of metastatic melanomas. Cancer Res. 2007;67(7):3064-73.
115. Hau P AR, Wiese P, Tschertner I, Blesch A, et al. Melanoma-inhibiting activity (MIA/CD-RAP) is expressed in a variety of malignant tumors of mainly neuroectodermal origin. Anticancer Res. 2002;22(2A):577-83.

116. Teodorczyk M, Schmidt MH. Notching on cancer's door: Notch signaling in brain tumors. Front Oncol. 2015;4:341.
117. Naka H, Nakamura S, Shimazaki T, Okano H. Requirement for COUP-TFI and II in the temporal specification of neural stem cells in CNS development. Nat Neurosci. 2008;11(9):1014-23.
118. Li D, Masiero M, Banham AH, Harris AL. The notch ligand JAGGED1 as a target for anti-tumor therapy. Front Oncol. 2014;4:254.
119. Xing F, Kobayashi A, Okuda H, Watabe M, Pai SK, et al. Reactive astrocytes promote the metastatic growth of breast cancer stem-like cells by activating Notch signalling in brain. EMBO Molecular Med. 2013;5(3):384-96.
120. Haupt S, Borghese L, Brustle O, Edenhofer F. Non-genetic modulation of Notch activity by artificial delivery of Notch intracellular domain into neural stem cells. Stem Cell Rev. 2012;8(3):672-84.
121. Qiu J, Takagi Y, Harada J, Topalkara K, Wang Y, et al. p27Kip1 constrains proliferation of neural progenitor cells in adult brain under homeostatic and ischemic conditions. Stem Cell. 2009;27(4):920-7.
122. Clevers H. The cancer stem cell: premises, promises and challenges. Nat Medicine. 2011;17(3):313-9.
123. Kim J, Lo L, Dormand E, Anderson DJ. SOX10 maintains multipotency and inhibits neuronal differentiation of neural crest stem cells. Neuron. 2003;38(1):17-31.
124. Okamura Y, Saga Y. Notch signaling is required for the maintenance of enteric neural crest progenitors. Development. 2008;135(21):3555-65.
125. Matsumata M, Sakayori N, Maekawa M, Owada Y, Yoshikawa T, et al. The effects of Fabp7 and Fabp5 on postnatal hippocampal neurogenesis in the mouse. Stem Cell. 2012;30(7):1532-43.
126. Jacob C, Lotscher P, Engler S, Baggiolini A, Varum Tavares S, et al. HDAC1 and HDAC2 control the specification of neural crest cells into peripheral glia. J Neurosci. 2014;34(17):6112-22.
127. Sarmento LM, Huang H, Limon A, Gordon W, Fernandes J, et al. Notch1 modulates timing of G1-S progression by inducing SKP2 transcription and p27 Kip1 degradation. J Exp Med. 2005;202(1):157-68.
128. Tirino V, Desiderio V, Paino F, De Rosa A, Papaccio F, et al. Cancer stem cells in solid tumors: an overview and new approaches for their isolation and characterization. FASEB J. 2013;27(1):13-24.
129. Capaccione KM, Pine SR. The Notch signaling pathway as a mediator of tumor survival. Carcinogenesis. 2013;34(7):1420-30.
130. Dohda T, Maljukova A, Liu L, Heyman M, Grander D, et al. Notch signaling induces SKP2 expression and promotes reduction of p27Kip1 in T-cell acute lymphoblastic leukemia cell lines. Exp Cell Res. 2007;313(14):3141-52.
131. Gao D, Inuzuka H, Tseng A, Chin RY, Toker A, et al. Phosphorylation by Akt1 promotes cytoplasmic localization of Skp2 and impairs APCCdh1-mediated Skp2 destruction. Nat Cell Bio. 2009;11(4):397-408.
132. Karbanova J, Laco J, Marzesco AM, Janich P, Vobornikova M. Human prominin-1 (CD133) is detected in both neoplastic and non-neoplastic salivary gland diseases and released into saliva in a ubiquitinated form. PLoS One. 2014;9(6):e98927.

133. Goto Y, Matsuzaki Y, Kurihara S, Shimizu A, Okada T, et al. A new melanoma antigen fatty acid-binding protein 7, involved in proliferation and invasion, is a potential target for immunotherapy and molecular target therapy. Cancer Res. 2006;66:4443.
134. Zhang H, Rakha EA, Ball GR, Spiteri I, Aleskandarany M, et al. The proteins FABP7 and OATP2 are associated with the basal phenotype and patient outcome in human breast cancer. Breast Canc Res Treat. 2010;121:41.
135. Chan CH, Morrow JK, Zhang S, Lin HK. Skp2: a dream target in the coming age of cancer therapy. Cell Cycle. 2014;13(5):679-80.
136. Lee SW, Li CF, Jin G, Cai Z, Han F, et al. Skp2-dependent ubiquitination and activation of LKB1 Is essential for cancer cell survival under energy stress. Mol Cell. 2015;57(6):1022-33.
137. Chan CH, Li CF, Yang WL, Gao Y, Lee SW, et al. The Skp2-SCF E3 ligase regulates Akt ubiquitination, glycolysis, herceptin sensitivity, and tumorigenesis. Cell. 2012;149(5):1098-111.

Figure 1

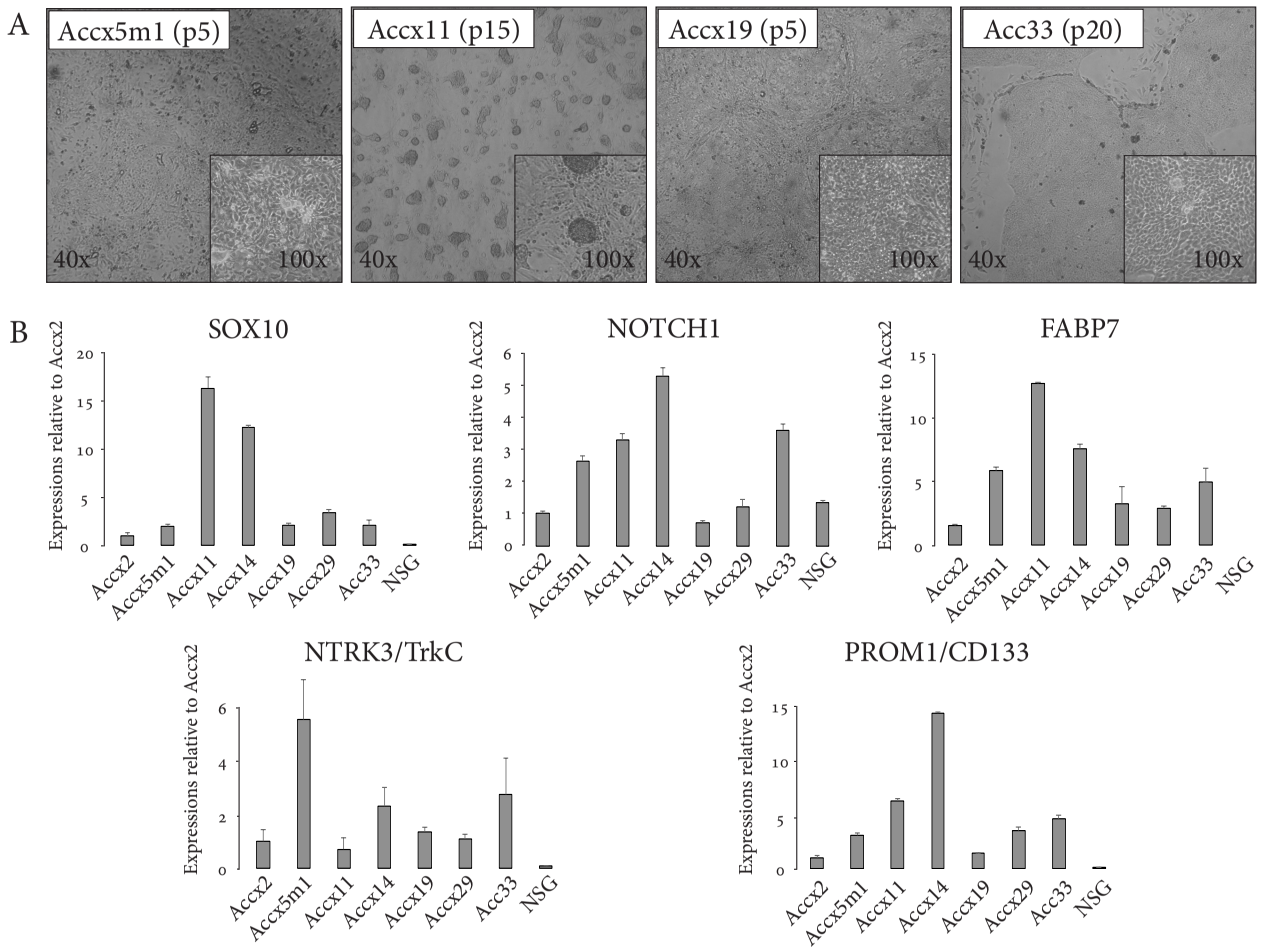

Figure 1. Cytological and molecular properties of ACC cell cultures.
(A) Low and high magnification brightfield images of cultured ACC cells at indicated passages for Accx5m1, Accx11, Accx19, and Acc33. (B) Real-time PCR quantification (RT-PCR) of gene expression for SOX10, NOTCH1, FABP7, NTRK3/TrkC, and PROM1/CD133 in cultured ACC cells compared to cultured cells isolated from normal salivary gland (NSG). In all RT-PCR experiments, expression is normalized to β-actin and error bars show standard errors representative of at least two independent experiments.

Figure 2

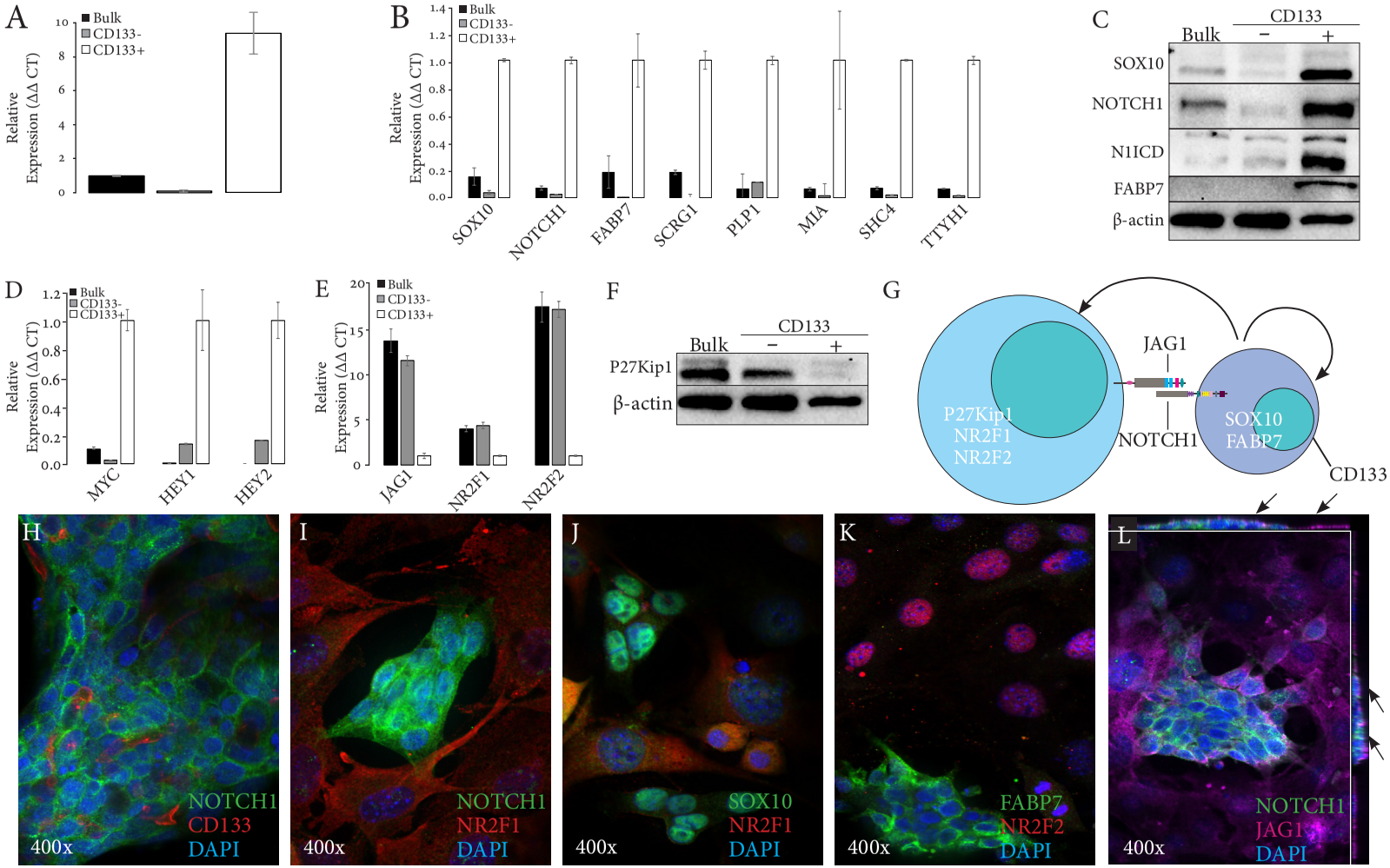
A
Bulk
CD133-
CD133+
Relative Expression (ΔΔ CT)
B
SOX10
NOTCH1
FABP7
SCRG1
PLP1
MIA
SHC4
TTYH1
C
Bulk
CD133
SOX10
NOTCH1
N1ICD
FABP7
β-actin
D
MYC
HEY1
HEY2
E
JAG1
NR2F1
NR2F2
F
P27Kip1
β-actin
G
P27Kip1
NR2F1
NR2F2
JAG1
NOTCH1
SOX10
FABP7
CD133
H
NOTCH1
CD133
DAPI
400x
I
NOTCH1
NR2F1
DAPI
J
SOX10
NR2F1
DAPI
K
FABP7
NR2F2
DAPI
L
NOTCH1
JAG1
DAPI

Figure 2. Isolation and characterization of CD133$^+$ and CD133$^-$ cells in Accx11 culture.
(A) RT-PCR of CD133 expression in Accx11 cell fractions following magnetic-activated cell sorting (MACS).
(B) Expression analysis by RT-PCR of ACC-associated (SOX10 & FABP7) and NSC-associated (NOTCH1, SCRG1, PLP1, MIA, SHC4, & TTYH1) genes in MACS-sorted Accx11 cell fractions.
(C) Immunoblot analysis shows selective expression of SOX10, NOTCH1, activated intracellular domain of Notch-1 (N1ICD), and FABP7 in CD133$^+$ cells. β-actin serves as a loading control.
(D) Expression analysis by RT-PCR of Notch targets MYC, HEY1, and HEY2 in MACS-sorted Accx11 cell fractions.
(E) Expression analysis by RT-PCR of JAG1 and neural differentiation markers NR2F1 and NR2F2 in MACS-sorted Accx11 cell fractions.
(F) Immunoblot analysis of CD133 fractions demonstrates CD133$^-$ cell-specific p27Kip1 expression. β-actin serves as a loading control.
(G) Molecular determinants of stem-like CD133$^+$ cells and more differentiated CD133$^-$ cells.
(H-L) Immunofluorescence staining demonstrates great selectivity of CD133$^+$ and CD133$^-$ cell markers and confirms spheroid-forming property of CD133$^+$ cells. Z-stack images (L) show NOTCH1 and JAG1 co-localization at sites of spheroidal and non-spheroidal cell contacts (arrows).

A

Tumor	CD133+
ACCX5M1	30%
ACCX6	50%
ACCX9	21%
ACCX11	43%
ACCX33	65%

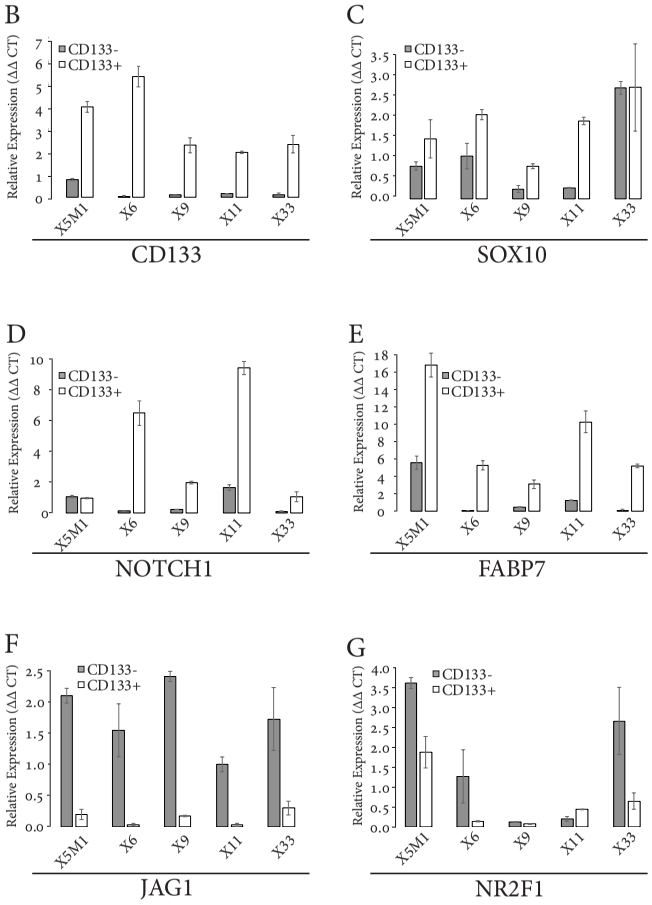

Figure 3. Isolation and characterization of CD133 fractions from ACC xenografts.

(A) Variation in the percentage of $CD133^+$ cells across ACC xenografts.

(B) RT-PCR analysis of CD133 expression confirms adequate separation of $CD133^+$ and $CD133^-$ cells isolated from ACC xenografts.

(C-E) Selectivity of SOX10, NOTCH1, and FABP7 to $CD133^+$ cells isolated directly from ACC xenografts as confirmed by RT-PCR.

(F, G) Selectivity of JAG1 and NR2F1 to $CD133^-$ cells isolated directly from ACC xenografts as confirmed by RT-PCR.

Figure 4

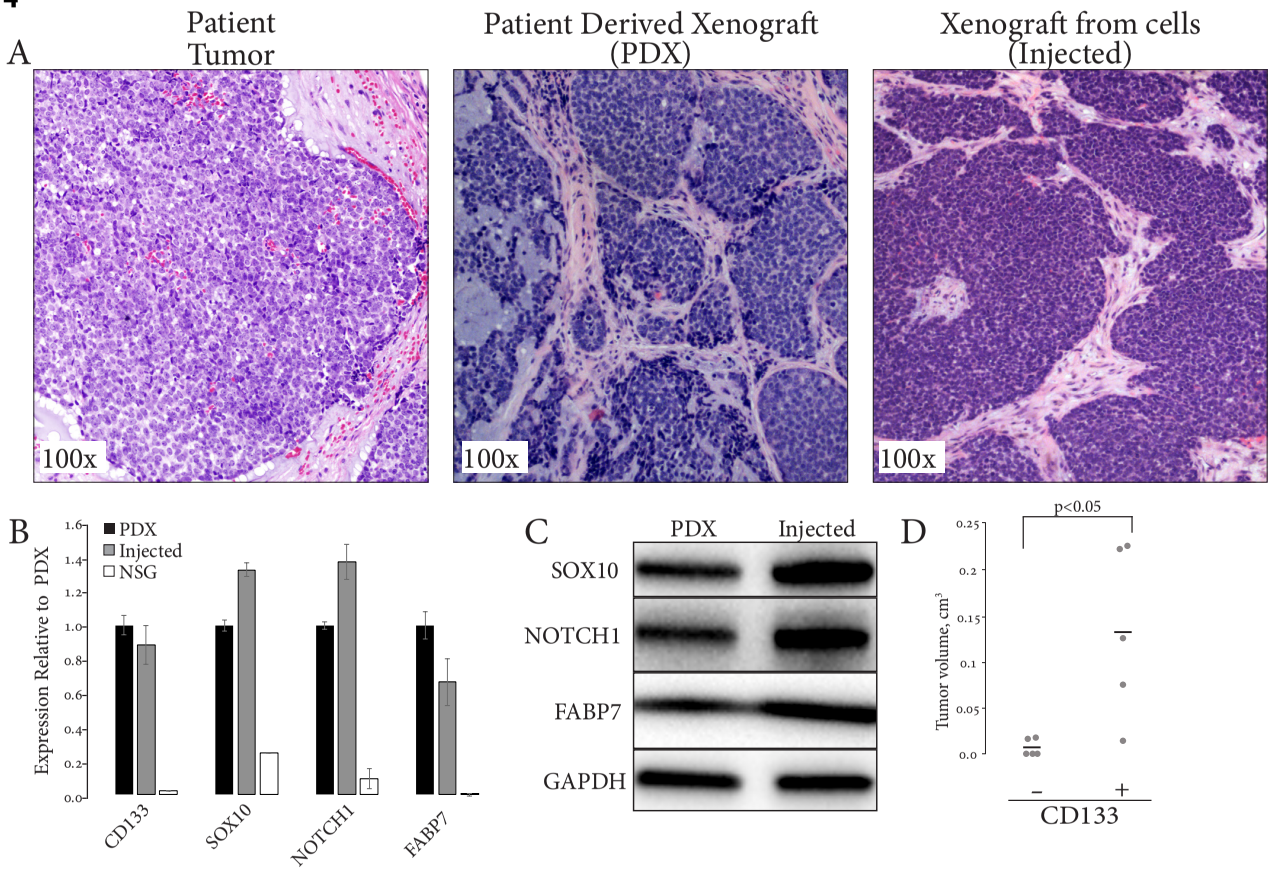

Figure 4. Tumorigenic properties of bulk and CD133-fractionated Accx11 cells.

(A) Cultured bulk Accx11 subcutaneously injected in athymic nude mice produce tumors with histology similar to patient tumor and parental xenograft (H&E staining).

(B) CD133, SOX10, NOTCH1, and FABP7 expression compared with normal salivary gland tissue (NSG) confirms ACC identity of PDX tumors and tumors generated from injection of bulk Accx11 cells.

(C) Immunoblot analysis confirms similar expression of SOX10, NOTCH1, and FABP7 in PDX and tumor formed from injected bulk Accx11 cells. GAPDH serves as a loading control.

(D) Dot plot of tumor volumes 13 weeks after injection of 10^5 $CD133^-$ or $CD133^+$ MACS-sorted Accx11 cells.

Figure 5

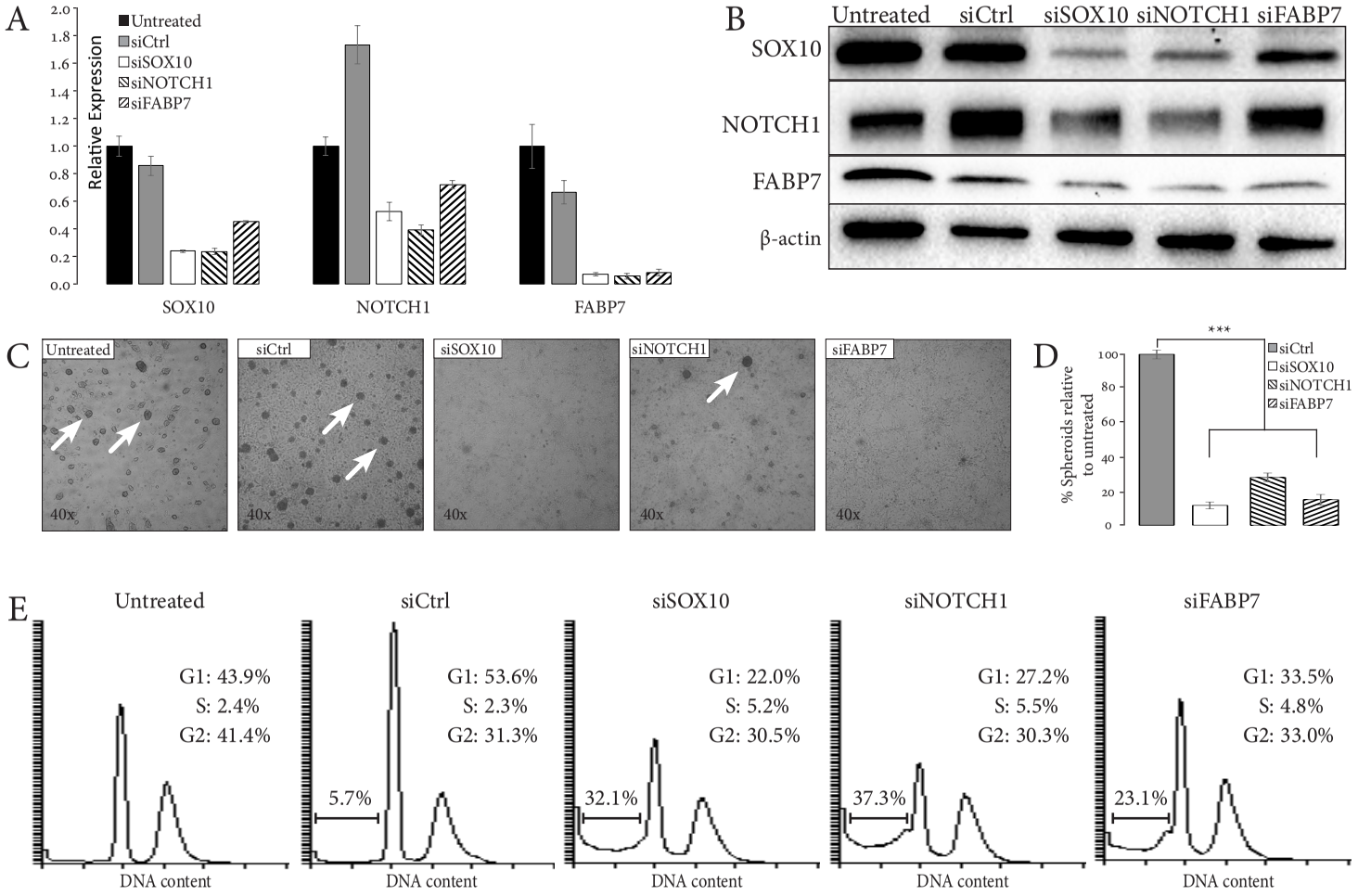
A
Relative Expression
Untreated
siCtrl
siSOX10
siNOTCH1
siFABP7
SOX10
NOTCH1
FABP7
B
Untreated
siCtrl
siSOX10
siNOTCH1
siFABP7
SOX10
NOTCH1
FABP7
β-actin
C
Untreated
siCtrl
siSOX10
siNOTCH1
siFABP7
40x
D
***
% Spheroids relative to untreated
siCtrl
siSOX10
siNOTCH1
siFABP7
E
Untreated
G1: 43.9%
S: 2.4%
G2: 41.4%
siCtrl
5.7%
G1: 53.6%
S: 2.3%
G2: 31.3%
siSOX10
32.1%
G1: 22.0%
S: 5.2%
G2: 30.5%
siNOTCH1
37.3%
G1: 27.2%
S: 5.5%
G2: 30.3%
siFABP7
23.1%
G1: 33.5%
S: 4.8%
G2: 33.0%
DNA content

Figure 5. Interrelated stimulatory effects of SOX10, NOTCH1, and FABP7 on ACC cells.
(A) RT-PCR analysis of SOX10, NOTCH1, and FABP7 expression following siRNA knockdowns reveals their regulatory interdependence.
(B) Validation of SOX10, NOTCH1, and FABP7 interdependence by Western blot. β-actin serves as a loading control.
(C) Depletion of SOX10, NOTCH1, and FABP7 by siRNA suppresses spheroidogenesis of Accx11 cells at 72 hours. Arrows: brightfield images of spheroids.
(D) Quantification of suppressive SOX10, NOTCH1, and FABP7 knockdown effects on spheroids compared to untreated Accx11 cells. Error bars represent standard errors and are representative of at least two independent experiments. In each case, siRNA knockdown resulted in a significant decrease in spheroid formation ($p<0.001$, Student's t-test).
(E) Suppression of SOX10, NOTCH1, and FABP7 by siRNA increases sub-G1 cell population indicative of cell death. Histograms represent cell counts based on propidium iodide (PI) staining of Accx11 cells. Percentages of live cells in different cell cycle phases are shown.

Figure 6

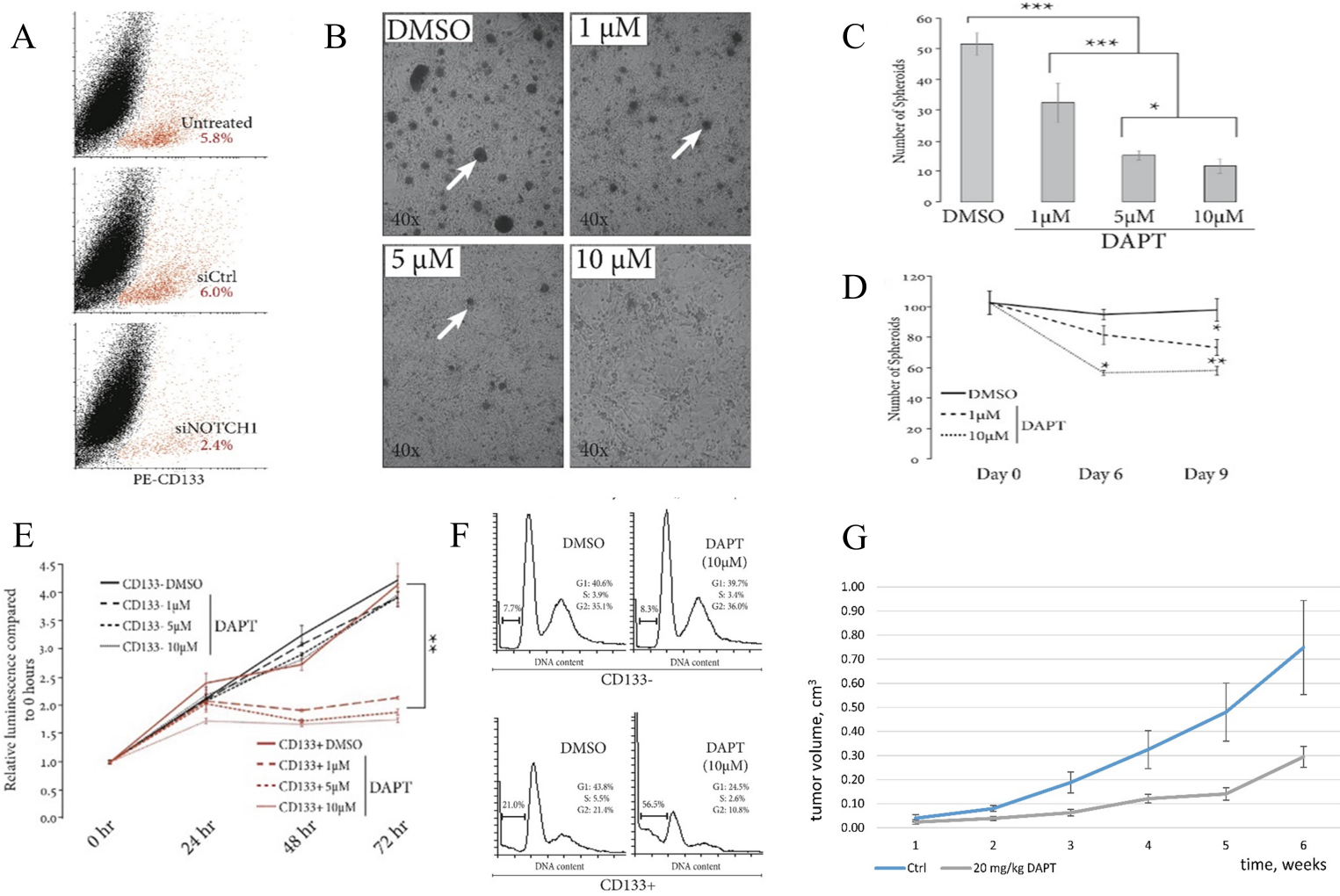
A
Untreated
5.8%
siCtrl
6.0%
siNOTCH1
2.4%
PE-CD133
B
DMSO
1 μM
5 μM
10 μM
40x
C
Number of Spheroids
DMSO
1μM
5μM
10μM
DAPT
D
Number of Spheroids
DMSO
1μM
10μM
DAPT
Day 0
Day 6
Day 9
E
Relative luminescence compared to 0 hours
CD133- DMSO
CD133- 1μM
CD133- 5μM
CD133- 10μM
DAPT
CD133+ DMSO
CD133+ 1μM
CD133+ 5μM
CD133+ 10μM
DAPT
0 hr
24 hr
48 hr
72 hr
F
DMSO
DAPT (10μM)
G1: 40.6%
S: 3.9%
G2: 35.1%
7.7%
G1: 39.7%
S: 3.4%
G2: 36.0%
8.3%
DNA content
CD133-
DMSO
DAPT (10μM)
G1: 43.8%
S: 5.5%
G2: 21.4%
21.0%
G1: 24.5%
S: 2.6%
G2: 10.8%
56.5%
DNA content
CD133+
G
tumor volume, cm3
time, weeks
Ctrl
20 mg/kg DAPT

Figure 6 (cont.)

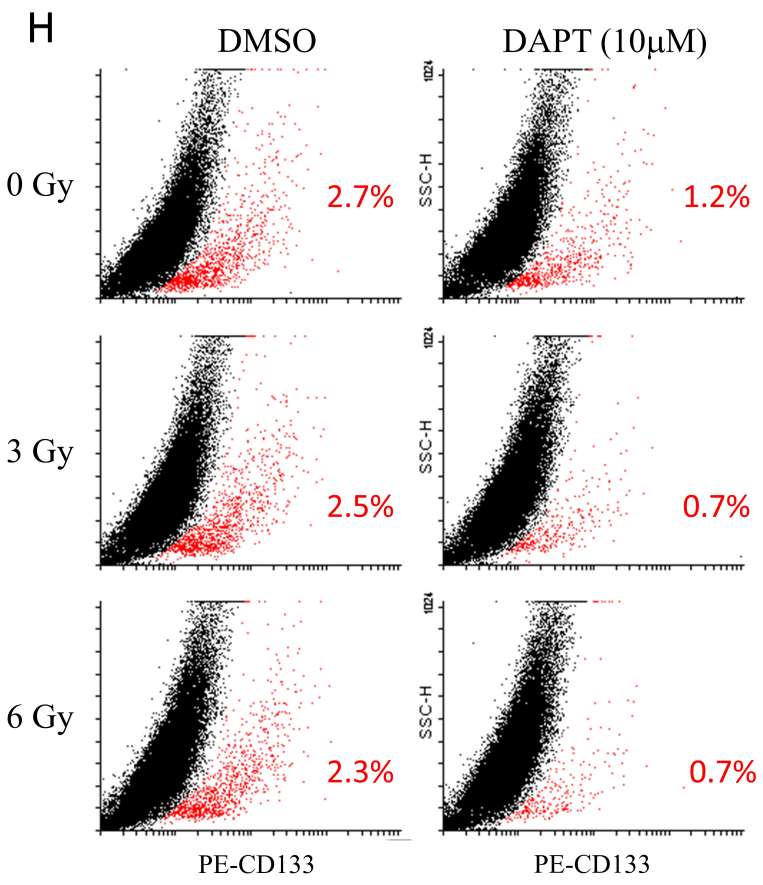

Figure 6. Inhibition of Notch signaling selectively depletes CD133⁺ cells.

(A) Suppression of NOTCH1 signaling by siRNA decreases the CD133⁺ cell fraction (red) as demonstrated by FACS analysis using PE-conjugated CD133 antibody.

(B) Inhibition of Notch signaling with gamma-secretase inhibitor DAPT demonstrates dose-dependent suppressive effects on spheroid formation (arrows) in Accx11 culture at 48 hours.

(C) Quantification of DAPT effects on spheroid formation compared to control (DMSO-treated) Accx11 cells.

(D) Breakdown of pre-formed spheroids induced by DAPT as shown by quantification of remaining spheroids following DAPT treatment versus control (DMSO-treated) Accx11 cells.

(E) Inhibitory DAPT effect on cell proliferation is highly CD133⁺-selective and dose-dependent. At 72 hours, there is a statistically significant decrease ($p<0.01$) in luminescence (Cell Titer Glo assay).

(F) DAPT selectively induces cell death in the CD133⁺ population as demonstrated by increase in sub-G1 cell population. Histograms represent cell counts based on PI-staining of separated Accx11 cells. $p<0.05$ (*), $p<0.01$ (**), $p<0.001$ (***), two-tailed t-test.

(G) Suppressive effect of DAPT on tumor growth in a nude mouse model subcutaneously injected with Accx11. Starting at week 2, $p<0.01$.

(H) Combination of DAPT with radiation is more detrimental to CD133⁺ cells (red) than DAPT or radiation alone. Representatives of 3 replicates are shown ($p<0.05$ in all comparisons except 3 Gy vs 6 Gy, radiation only). FACS analysis was performed with PE-conjugated CD133 antibody.

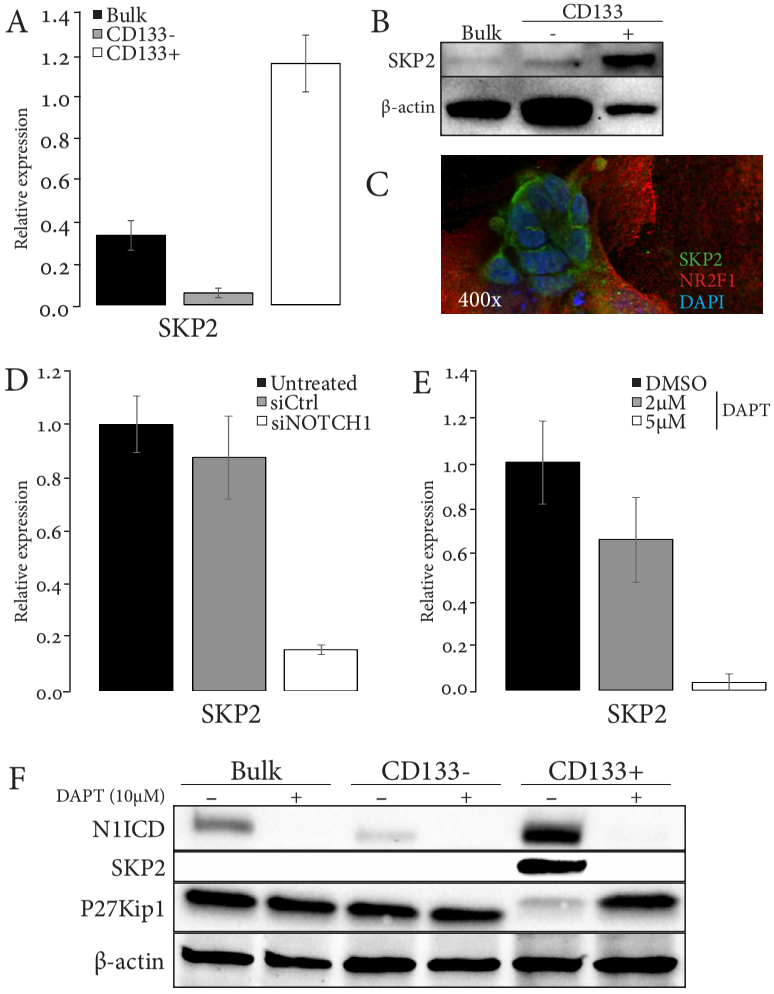

Figure 7. CD133$^+$-cell-selective and NOTCH1-dependent SKP2 expression in ACC cells.

(A-C) SKP2 is selectively expressed in CD133$^+$ Accx11 cells as demonstrated by RT-PCR (A), immunoblot (B), and shows cytoplasmic localization in spheroid-forming CD133$^+$ cells as demonstrated by immunofluoresence (C). β-actin serves as a control for (A) and (B).

(D-E) Inhibition of Notch signaling by siRNA (D) and DAPT (E) decreases expression of SKP2 in bulk Accx11 cells (RT-PCR).

(F) DAPT blocks expression of activated NOTCH1 (N1ICD) and its target SKP2 in CD133$^+$ ACC cells and up-regulates p27Kip1, a SKP2 substrate. β-actin serves as a loading control.

Supplemental Figure 1

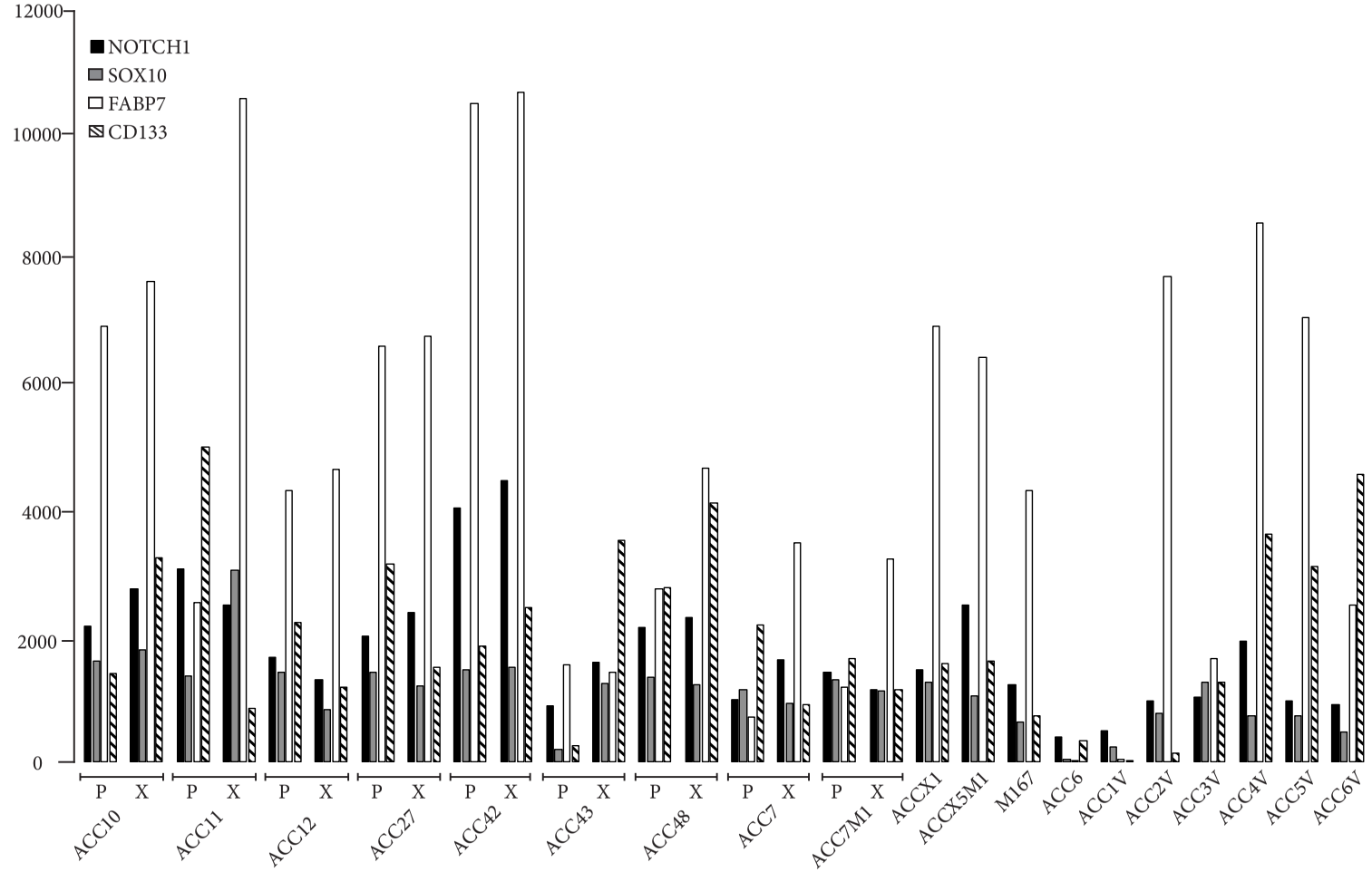

Supplemental Figure 1. Expression of SOX10, NOTCH1, FABP7, and CD133 in ACC tumor specimens from patients (P) and PDX (X). The comparison is based on previously produced Affymetrix data (110).

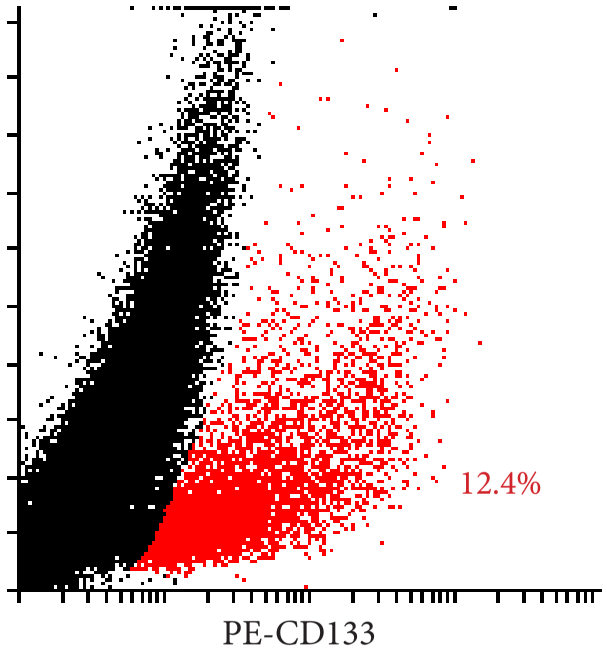

Supplemental Figure 2. FACS analysis of Accx11 cells stained with PE-conjugated CD133 antibody.
CD133+ cells (red) comprise ~12.4% of the bulk population.

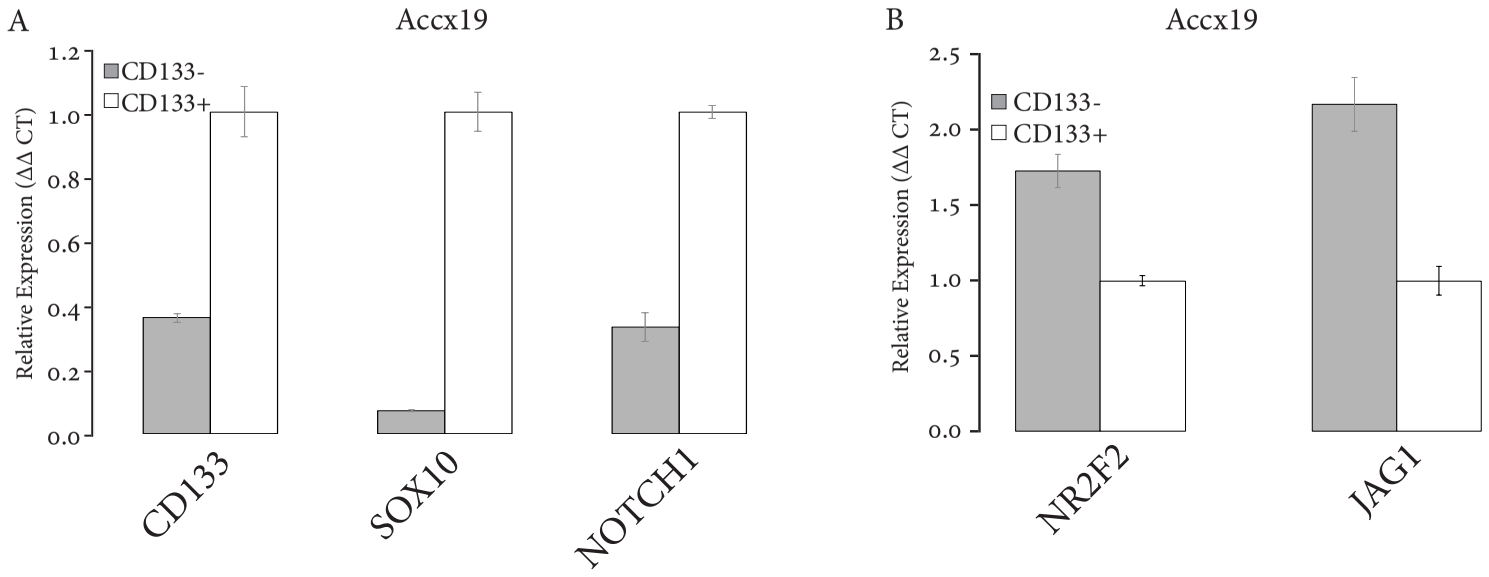

Supplemental Figure 3. FACS analysis of Accx19 cells stained with PE-conjugated CD133 antibody.
Expression analysis of Accx19 cultured cells by RT-PCR demonstrates enrichment of $CD133^{+}$ markers (A) and $CD133^{-}$ markers (B), similar to the pattern seen in Accx11 cells. Expression is normalized to β-actin and error bars are standard error representative of at least two independent experiments.

Supplemental Figure 4

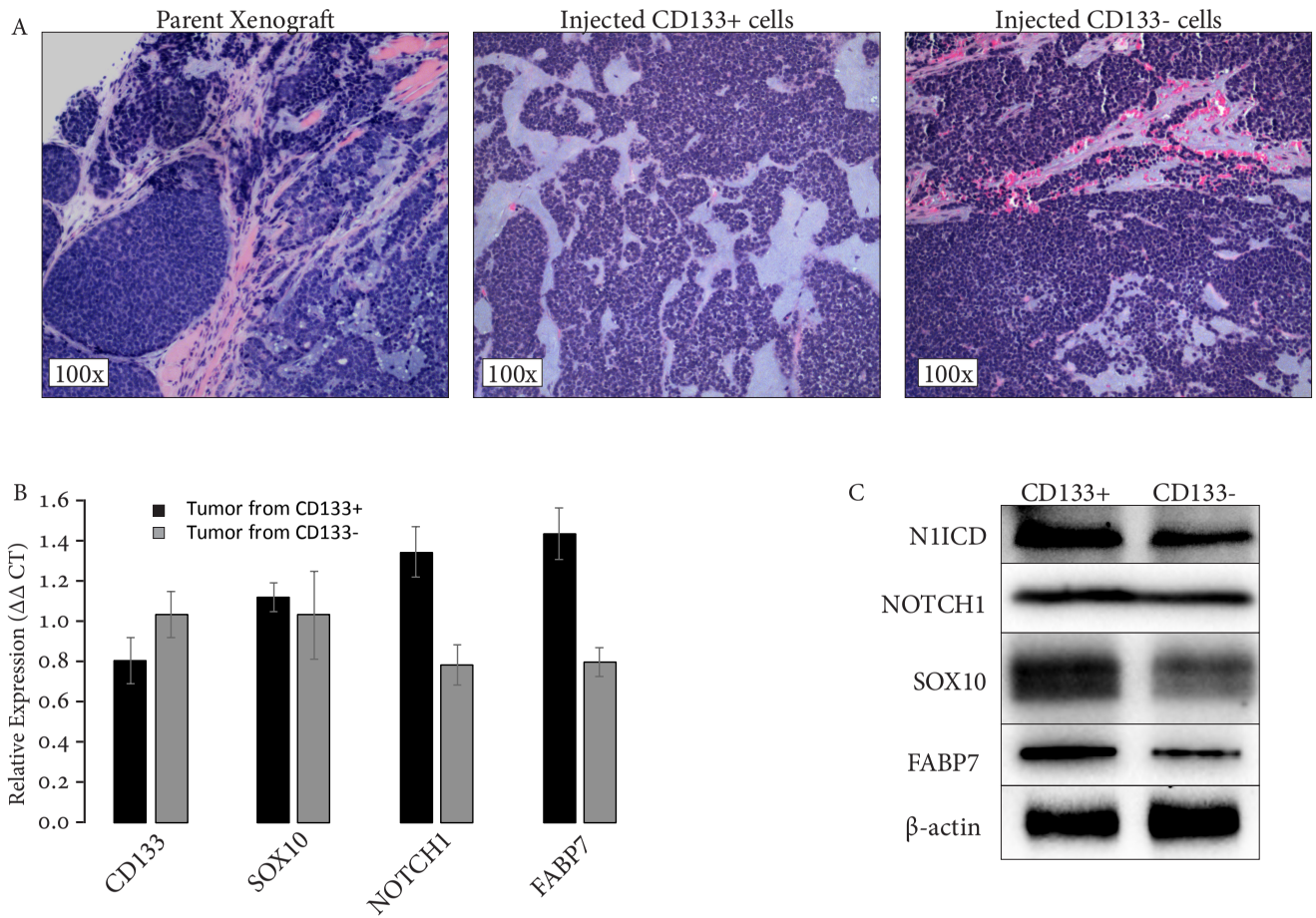

Supplemental Figure 4. Tumors formed from injected Accx11 CD133$^-$ cells closely parallel tumors formed from injected CD133+ cells.

Analysis of histological grade by H&E staining (A), gene expression by RT-PCR (B), and protein expression by immunoblot (C). β-actin serves as a control for all experiments. Error bars represent standard error representative of at least two experiments.

Supplemental Figure 5

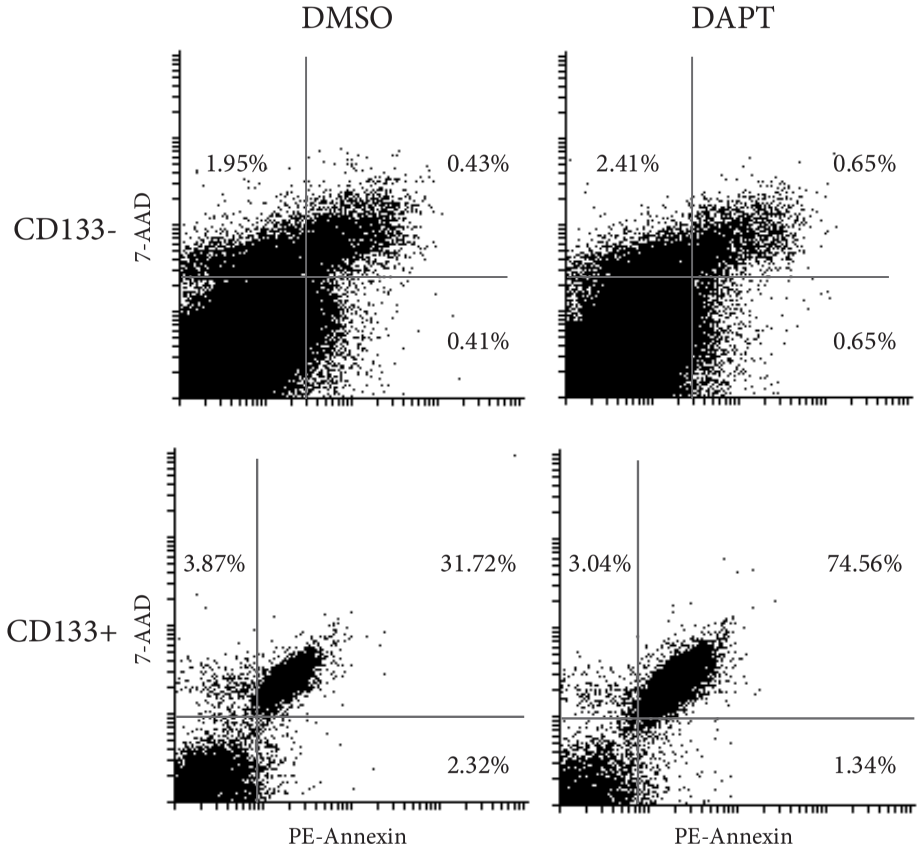

Supplemental Figure 5. DAPT selectively increases cell death in CD133^{+} Accx11 cells as shown by PE-annexin and 7-AAD double staining.
DMSO treatment serves as a control.

Table 1. Characteristics of ACC cultures and their parental tumors.

Cell Culture ID	Tumor grade	Histology	Max Passage	Doubling Time (hrs)
Accx5m1	2M	Cribriform	8	77
Accx11	3	Solid	>30	29
Accx14	1	Cribriform	15	96
Accx19	2	Cribriform	10	86
Accx29	1	Unknown	18	60
Acc33	2	Cribriform & Tubular	>30	84

Table 2. Validation of ACC cell culture via microsatellite analysis of eight STR sites.

Sample	Xenograft or Cx	TH01	D21S11	D5S818	D13S317	D7S820	D16S539	CSF1PO	Amelogenin
ACCX2	Xenograft	10	28.3, 31, 32	10.1, 11.1	11, 12, 15	11	11, 12.1	11, 12	-
Accx2	Culture	10	27.3, 28.3, 30.3, 31.2	10.1, 11.1, 12.3	11, 13, 14	8, 11	10, 11, 12.1	6.3, 11, 12	X
ACCX5M1	Xenograft	9.1, 10	28, 29.3, 32, 32.1	12.3	10, 14	7, 11	9, 11	9.3, 11	X, Y
Accx5M1	Culture	9.1, 10	29.3, 32.1	12.3	11, 14	7, 11	9, 13.1	9.3, 10.3	X, Y
ACCX11	Xenograft	6.1, 10	28.3, 31.1	11.1	13, 14,	8, 9.1	11, 12.1,	10, 12	X
Accx11:9	Culture	6.1, 10	28.3, 31.1	11.1	13, 14,	8, 9.1	11, 12.1,	10, 12	X
ACCX11:9p:0	Xenograft from Cx	6.1, 10	28.3, 31.1	-	13, 14,	8, 9.1	11, 12.1,	10, 12	X
ACCX11 CD133-	Xenograft from Cx	6.1, 10	28.3, 31.1	11.1	13, 14	8, 9	11, 13	10, 12	X
ACCX11 CD133+	Xenograft from Cx	6.1, 10	28.3, 30, 31.1	11.1	13, 14	8, 9	11, 13	10, 12	X
ACCX14:9	Xenograft	8, 10, 13.3	28.3	10.1, 11	15	9, 10	12.1	11, 12	X
Accx14:9	Culture	8.3, 10	28.3	10.1, 11.1	14	9.1, 10	11, 12.1	11, 12	X
ACCX19	Xenograft	7.1, 8	27.3	12.3	13, 15	8, 11	10, 11	6.3, 12	-
Accx19	Culture	7.1, 8	27.3	12.3	13, 15	8, 11	10, 11	6.3, 12	-
ACCX29	Xenograft	6.1, 7.1	29.3, 31	10.1, 11	13, 14	10	9, 11	12	X
Accx29	Culture	6.1, 7.1	29.3, 31.1	10.1, 11.1	13, 15	9.3,	9, 11	12,	X
ACC33	Xenograft	9.1, 10	28.3, 29.3	9	11, 15	9.3, 11	11, 12.1	11, 14	X
Acc33	Culture	9.1, 10	28.3, 29.3	9	10, 14	10, 11	11, 12.1	11, 14	X

Table 3. Genes and pathways suppressed by FABP7 knockdown in Accx11 cells.

Pathway/Gene Signature	# Genes	Gene Name	Statistics, p value
Cell cycle	31	ANAPC7, BUB1, BUB1B, CCNA2, CCNB2, CCND1, CCNE2, CDC20, CDC6, CDK1, CDK4, CDK6, CDKN2C, CHEK1, DBF4, MAD2L1, MCM2, MCM3, MCM4, MCM6, MYC, ORC5, PRKDC, PTTG1, **SKP2**, TFDP1, TFDP2, TGFB2, TTK	2.19E-22
Ribosome	27	RPL0, RPL3, RPL4, RPL5, RPL6, RPL7A, RPL10, RPL10A, RPL13, RPL13A, RPL14, RPL15, RPL22, RPL23, RPL27A, RPL31, RPL35A, RPL37, RPS2, RPS3, RPS6, RPS7, RPS8, RPS15A, RPS20, RPS21, RPS23	1.08E-21
Metabolic pathways	82	ACAT1, ACO1, ACOX1, ACY1, ADI1, ADSL, AGPS, AHCY, ALDH5A1, ALDH6A1, ALDH7A1, ALG10B, ALG13, ALG9, ARG2, ATP5G2, ATP6V0E2, BCAT2, COX15, COX17, CPS1, CTH, DBT, DHFR, DPM3, DTYMK, DUT, ENO1, EPT1, ETNK1, FECH, FH, GFPT1, GLCE, GLS, GOT1, GPAM, GPAT2, HADH, HADHA, HSD17B1, HSD17B2, IDH2, IMPDH2, KDSR, LTA4H, MGAT4A, MTHFD1, MTHFD2, MTHFD2L, MTR, ODC1, PAICS, PFAS, PGM2, PHGDH, PIGK, PIGN, PLA2G12A, POLA1, POLD2, POLE3, POLE4, POLR2J, PRIM1, PRIM2, PTDSS1, PTGES, PTGIS, PYCR2, QARS, RRM1, RRM2, SEPHS1, TK1, TKT, TUSC3, TYMS, UQCRB, UQCRH, UQCRQ, ZNRD1	8.47E-18
NOTCH1	11	CCND1, ENO1, HES6, HEY1, HEY2, JAG1, MIB1, MYC, NOTCH1, **SKP2**, YY1	2.30E-05
SOX10 ACC signature	26	ABI2, ACTR3B, CADM1, CCNB1IP1, CHDH, DPY19L2, EPHA7, FGFR2, FRMD4A, GPM6B, ITGA9, LGR6, MTL5, MYEF2, NLN, NRCAM, NRTN, PPP1R1B, RAP2A, RPL3, SEPT4, SHANK2, SLC35F3, TEX261, TMEM63A, TTC3	1.40E-12